

# Stable Models and Temporal Difference Learning

Gaurav Manek

CMU-CS-23-103

April 2023

Computer Science Department  
School of Computer Science  
Carnegie Mellon University  
Pittsburgh, PA 15213

**Thesis Committee:**

J. Zico Kolter, Chair

David Held

Deepak Pathak

Sergey Levine (UC Berkeley)

*Submitted in partial fulfillment of the requirements  
for the degree of Doctor of Philosophy.*

Copyright © 2023 **Gaurav Manek**

This research was sponsored by Agency for Science, Technology and Research (A\*STAR) Singapore and Robert Bosch GmbH

The views and conclusions contained in this document are those of the author and should not be interpreted as representing the official policies, either expressed or implied, of any sponsoring institution, the U.S. government or any other entity.

**Keywords:** Lyapunov Stability, Regularization, Deadly Triad, Offline Reinforcement Learning, Temporal Difference Learning, Reinforcement Learning, Neural Networks, Machine Learning, Artificial Intelligence

## Abstract

In this thesis, we investigate two different aspects of stability: the stability of neural network dynamics models and the stability of reinforcement learning algorithms. In the first chapter, we propose a new method for learning Lyapunov-stable dynamics models that are stable by construction, even when randomly initialized. We demonstrate the effectiveness of this method on damped multi-link pendulums and show how it can be used to generate high-fidelity video textures.

In the second and third chapters, we focus on the stability of Reinforcement Learning (RL). In the second chapter, we demonstrate that regularization, a common approach to addressing instability, behaves counterintuitively in RL settings. Not only is it sometimes ineffective, but it can also cause instability. We demonstrate this phenomenon in both linear and neural network settings. Further, standard importance sampling methods are also vulnerable to this.

In the third chapter, we propose a mechanism to stabilize off-policy RL through resampling. Called Projected Off-Policy TD (POP-TD), it resamples TD updates to come from a convex subset of “safe” distributions instead of (as in other resampling methods) resampling to the on-policy distribution. We show how this approach can mitigate the distribution shift problem in offline RL on a task designed to maximize such shift.

Overall, this thesis advances novel methods for dynamics model stability and training stability in reinforcement learning, questions existing assumptions in the field, and points to promising directions for stability in model and reinforcement learning.



## Acknowledgments

Although it is not possible to express my gratitude to everyone who has played a role in my academic and personal growth, I want to acknowledge and appreciate the countless friends, family, and collaborators whose contributions have been invaluable to me.

First and foremost, my advisor Zico Kolter. His guidance, advice, enthusiasm, expertise, encouragement, and unwavering support have been invaluable to me throughout this journey. His involvement has helped me develop a deeper understanding of the subject matter and how to approach research in a meaningful way. I also wish to thank Sergey Levine, David Held, and Deepak Pathak, for their invaluable feedback, suggestions, and guidance as members of my thesis committee.

I would like to express my sincere appreciation to my collaborators on the POP-TD project Melrose Roderick and Felix Berkenkamp, for their insight, good humor, time, patience, and tenacity.

From the department, I wish to thank Ruben Martins for engaging with my fledgeling ideas in his field. Also, the support staff who make the department what it is: Catherine Copetas, Deb Cavlovich, Ann Stetser, Charlotte Yano, and the many, many others. I also owe a debt of gratitude to Francisco Maturana, my roommate of six years, colleague in the CS department, and friend.

From A\*STAR, I wish to thank the many people in the past and present who have molded me as researchers and supported me through my PhD, especially Vijay Chandrasekhar and Li Xiaoli. I also wish to thank the many senior researchers who have invested their time in me, and the dedicated scholarship officers who have supported me for a decade. From my undergraduate years in Brown I need to thank Shriram Krishnamurthi and Stefanie Tellex for starting me down this journey.

And most of all, I would like to express my heartfelt thanks to my parents Mukesh and Sonal Manek, my brother Gautam Manek, and my extended family for their unwavering love, encouragement, and support throughout the highs and lows of my academic journey. Their steadfast presence, undying love, and unwavering support have been the foundation upon which I have built my academic success, and I am forever indebted to them.

# Contents

<b>Introduction</b>	<b>ix</b>
<b>1 Learning Stable Dynamics Models</b>	<b>1</b>
1.1 Introduction . . . . .	2
1.2 Background and related work . . . . .	3
1.3 Joint learning of dynamics and Lyapunov functions . . . . .	6
1.3.1 Properties of the Lyapunov function . . . . .	7
1.4 Empirical results . . . . .	11
1.4.1 Random networks . . . . .	12
1.4.2 n-link pendulum . . . . .	12
1.4.3 Video Texture Generation . . . . .	14
1.5 Conclusion . . . . .	16
1.6 Adaptation to Stable Control and RL . . . . .	16
<b>2 The Pitfalls of Regularization in Off-Policy TD</b>	<b>19</b>
2.1 Introduction . . . . .	20
2.2 Preliminaries and Notation . . . . .	23
2.3 Our Counterexamples . . . . .	26
2.3.1 Regularization cannot always mitigate the error from training off-policy. . . . .	26
2.3.2 Small amounts of regularization can cause large increases in training error. . . . .	33

2.3.3	Emphatic approaches and our counterexample . . . . .	35
2.3.4	Applied to multi-layer networks . . . . .	43
2.3.5	Over-parameterization does not solve this problem . . . . .	46
2.4	Related Work . . . . .	46
2.5	Relationship to modern RL algorithms . . . . .	49
2.6	Conclusion . . . . .	49
<b>3</b>	<b>Projected Off-Policy TD for Offline Reinforcement Learning</b>	<b>53</b>
3.1	Introduction . . . . .	54
3.2	Related Work . . . . .	55
3.3	Problem Setting and Notation . . . . .	57
3.3.1	The Non-Expansion Criterion (NEC) . . . . .	58
3.4	Projected Off-Policy TD (POP-TD) . . . . .	60
3.4.1	I- and M-projections . . . . .	61
3.4.2	Optimizing the distribution . . . . .	61
3.4.3	The structure of $Z$ . . . . .	62
3.4.4	Update rules . . . . .	64
3.4.5	POP-Q-Learning . . . . .	65
3.5	Experiments and Discussion . . . . .	67
3.5.1	POP-Q on GridWorld . . . . .	68
3.6	Conclusion . . . . .	71
	<b>Conclusion</b>	<b>75</b>
	<b>Notation and Definitions</b>	<b>77</b>
	<b>Bibliography</b>	<b>78</b>

# 1 Introduction

2 In this thesis we examine two notions of stability: that of neural network dynamics  
3 models and the training of reinforcement learning algorithms. There is a natural  
4 transition from the first notion of stability to the second is natural: the parameters  
5 of a stably trained model circumscribes, in parameter-space, a stable trajectory. This  
6 relationship between stabilities has significant precedence in the foundational work of  
7 Temporal Difference (TD) learning theory [54].

8 In the first chapter we propose a new method for learning Lyapunov-stable dynamical  
9 models and the certifying Lyapunov function in a fully end-to-end manner. Instead  
10 of enforcing stability by some loss function, we guarantee stability everywhere by  
11 construction. This works by carefully constructing a neural network to act as a  
12 Lyapunov function, learning a separate, unconstrained dynamics model, and then  
13 combining these two models with a novel reprojection layer. This produces models  
14 that are guaranteed stable by construction everywhere in the state space, even without  
15 any training. We show that such learning systems are able to model simple dynamical  
16 systems such as pendulums, and can be combined with additional deep generative  
17 models to learn complex dynamics, such as video textures, in a fully end-to-end  
18 fashion.

19 In modern Reinforcement Learning, TD is combined with function approximation  
20 (i.e. neural networks) and off-policy learning. However, these three are known as the  
21 *deadly triad* [48, p. 264], because they may cause severe instability in the learning  
22 process Tsitsiklis and Van Roy [54]. While many variants of TD will provably converge

23 despite the training instability, the quality of the solution at convergence is typically  
24 arbitrarily poor [24]. In the literature, there is a general belief that regularization can  
25 mitigate this instability, which is supported by basic analysis on the three standard  
26 examples.

27 However, this is not true! In the second chapter, we introduce a series of new  
28 counterexamples that are resistant to regularization. We demonstrate the existence  
29 of “vacuous” examples, which never do better than the limiting case regardless of the  
30 amount of regularization. This problem persists in most TD-based algorithms, which  
31 covers a wide swath of the RL literature; we make our analysis concrete by showing  
32 how this example forces the error bounds derived by Zhang, Yao, and Whiteson [63]  
33 to be extremely loose in practice. We further demonstrate that regularization is not  
34 monotonic in TD contexts, and that it is possible for regularization to increase error  
35 (or cause divergence) around some critical values. We extend these examples to the  
36 neural network case showing that these effects are not limited to the linear case and  
37 making the case for greater care in regularization in practical RL applications. Finally,  
38 there is a line of work starting with Emphatic-TD which seeks to stabilize off-policy  
39 training by resampling TD updates to appear on-policy. Contemporary Emphatic  
40 algorithms generally use a reversed version of TD to estimate the resampling function,  
41 which opens them up to instability from the same source as the original TD. We show  
42 that these techniques are similarly vulnerable. We show that regularization is not a  
43 panacea for stability in TD learning.

44 In the third chapter, we investigate new methods for stable TD learning that are  
45 resistant to off-policy divergence. Starting from an idea introduced by Kolter [24] we  
46 derive Projected Off-Policy TD, which reweighs TD updates to the closest distribution  
47 where the TD is non-expansive at the fixed point of its training. We learn the  
48 reweighing factors in the training loop using stochastic gradient descent (i.e. with  
49 time- and space-complexity comparable to learning the value function) and then  
50 apply those reweighing factors to each TD update. Crucially, this is distinct from  
51 contemporary work in the literature in that POP-TD does not resample to on-policy  
52 distribution, instead finding a “safe” distribution close to the data distribution.

53 Applying this to a novel offline RL example, we can clearly demonstrate how POP-  
54 TD mitigates the *distributional shift* between the dataset and the learned policy [30]  
55 while resampling as little as possible.

56 We conclude with a discussion on future directions that our work on stable models  
57 may take.



# 58 Chapter 1

## 59 Learning Provably Stable Deep 60 Dynamics Models

61 Deep networks are commonly used to model dynamical systems, predicting how the  
62 state of a system will evolve over time (either autonomously or in response to control  
63 inputs). Despite the predictive power of these systems, it has been difficult to make  
64 formal claims about the basic properties of the learned systems. In this chapter, we  
65 propose an approach for learning dynamical systems that are guaranteed to be stable  
66 over the entire state space. The approach works by jointly learning an unconstrained  
67 dynamics model and Lyapunov function, then combining them in a novel reprojection  
68 layer to produce models that are guaranteed to be stable by construction everywhere  
69 in the state space, even without any training. We show that such learning systems are  
70 able to model dynamical systems such as compound pendulums and can be combined  
71 with additional deep generative models to learn to generate images with complex  
72 dynamics such as video textures.

73 *From “Learning Stable Deep Dynamics Models” by Manek and Kolter (2019)*

## 74 1.1 Introduction

75 This chapter deals with the task of learning continuous-time dynamical systems.

76 Given  $x(t) \in \mathbb{R}^n$ , a state at time  $t$ , we wish to model the time-derivative

$$77 \quad \dot{x}(t) \equiv \frac{d}{dt}x(t) = f(x(t)) \quad (1.1)$$

78 for some function  $f : \mathbb{R}^n \rightarrow \mathbb{R}^n$ . Modeling the time evolution of such dynamical  
79 systems (or with control inputs  $\dot{x}(t) = f(x(t), u(t))$  for  $u(t) \in \mathbb{R}^m$  and  $f : \mathbb{R}^n \times \mathbb{R}^m \rightarrow$   
80  $\mathbb{R}^n$ ) is a foundational problem in machine learning, with applications in reinforcement  
81 learning, control, forecasting, and many other settings. Owing to their representational  
82 power, neural networks have long been a natural choice for modeling the function  
83  $f$  [14, 41, 37, 12]. However, when using a neural network to model dynamics in  
84 this setting very little can be guaranteed about the behavior of the learned system,  
85 especially about its stability. Informally, we say that a model is stable if we can  
86 pick a bounded set of states and guarantee that once the model enters that set it  
87 never leaves. While some recent work has begun to consider stability properties of  
88 neural networks [6, 45, 51], it has typically done so by softly enforcing stability as an  
89 additional loss term on the training data. Consequently, they can say little about the  
90 stability of the system in states outside the training data.

91 In this chapter, we propose an approach to learning neural network dynamics that are  
92 provably Lyapunov-stable over the entirety of the state space. We do this by jointly  
93 learning a nominal system dynamics and the certifying Lyapunov function, and then  
94 reprojecting the predictions of the nominal model onto the level set of the Lyapunov  
95 function. This stability is a hard constraint imposed upon the model: unlike recent  
96 approaches, we do not enforce stability via an imposed loss function but build it  
97 directly into the dynamics of the model. This means that even a randomly initialized  
98 model in our proposed model class will be provably stable everywhere in state space.  
99 The key to this is the design of a proper Lyapunov function, based on input convex  
100 neural networks [1], which ensures global exponential stability to an equilibrium point  
101 while still allowing for rich dynamics.

102 Using these methods, we demonstrate learning dynamics of physical models such as  
 103  $n$ -link pendulums, and show a substantial improvement over generic networks. We  
 104 also show how such dynamics models can be integrated into larger network systems to  
 105 learn dynamics over complex output spaces, combining the model with a variational  
 106 auto-encoder (VAE) [23] to learn dynamic video textures [46].

## 107 1.2 Background and related work

108 **Stability of dynamical systems.** We consider the setting of uncontrolled<sup>1</sup> dy-  
 109 namics systems  $\dot{x}(t) = f(x(t))$  for  $x(t) \in \mathbb{R}^n$ . Such a system is *globally asymptotically*  
 110 *stable* around the equilibrium point  $x_e = 0$  if we have  $x(t) \rightarrow 0$  as  $t \rightarrow \infty$  for any  
 111 initial state  $x(0) \in \mathbb{R}^n$ ;  $f$  is *locally asymptotically stable* if the same holds but only  
 112 for  $x(0) \in \mathcal{B}$  where  $\mathcal{B}$  is some bounded set containing the origin. Similarly,  $f$  is  
 113 *globally* or *locally* exponentially stable if trajectories approach to the origin is at some  
 114 minimum rate:

$$115 \quad \|x(t)\|_2 \leq m \|x(0)\|_2 e^{-\alpha t} \quad (1.2)$$

116 for some constants  $m, \alpha \geq 0$  for any  $x(0) \in \mathbb{R}^n$  ( $\mathcal{B}$ , respectively).

117 The area of Lyapunov theory [20, 29] establishes the connection between these types  
 118 of stability according to a *Lyapunov function*. Specifically, let  $V : \mathbb{R}^n \rightarrow \mathbb{R}$  be a  
 119 continuously differentiable positive definite function, i.e.,  $V(x) > 0$  for  $x \neq 0$  and  
 120  $V(0) = 0$ . Lyapunov analysis says that  $f$  is asymptotically stable, if and only if  
 121 there exists some function  $V$  as above such the value of this function decreases along  
 122 trajectories generated by  $f$ . Formally, this is the condition that the time derivative  
 123  $\dot{V}(x(t)) < 0$ , i.e.,

$$124 \quad \dot{V}(x(t)) \equiv \frac{d}{dt} V(x(t)) = \nabla V(x)^T \frac{d}{dt} x(t) = \nabla V(x)^T f(x(t)) < 0 \quad (1.3)$$

125 This condition must hold for all  $x(t) \in \mathbb{R}^n$  or for all  $x(t) \in \mathcal{B}$  to ensure global or local

<sup>1</sup>We will discuss extending this to dynamics with control later; this is a non-trivial extension.

126 stability respectively. Similarly  $f$  is globally exponentially stable if and only if there  
127 exists positive definite  $V$  with a sufficiently steep gradient such that

$$128 \quad \dot{V}(x(t)) \leq -\alpha V(x(t)), \quad \text{with } c_1 \|x\|_2^2 \leq V(x) \leq c_2 \|x\|_2^2. \quad (1.4)$$

129 Showing that these conditions imply the various forms of stability is relatively  
130 straightforward, but it is also true (but more complex to show) that any stable system  
131 must obey this property for some  $V$ . In this chapter our broad strategy is to construct  
132 a Lyapunov function and enforce conditions that ensure stability.

133 **Stability of linear systems.** For a linear system with matrix  $A$

$$134 \quad \dot{x}(t) = Ax(t) \quad (1.5)$$

135 it is well-known that the system is stable if and only if the real components of the  
136 the eigenvalues of  $A$  are all strictly negative. Equivalently, the same same property  
137 can be shown via a positive definite quadratic Lyapunov function

$$138 \quad V(x) = x^T Q x \quad (1.6)$$

139 for  $Q \in \mathbb{R}^{n \times n}, Q \succ 0$ . In this case, by Equation 1.4, the following ensures global  
140 exponential stability:

$$141 \quad \dot{V}(x(t)) = x(t)^T A^T Q x(t) + x(t)^T Q A x(t) \leq -\alpha x(t)^T Q x(t) \quad (1.7)$$

142 i.e., if we can find a positive definite matrix  $Q \succeq I$  such that  $A^T Q + Q A + \alpha Q \preceq 0$   
143 negative semidefinite. Such bounds (and much more complex extensions) for the  
144 basis for using linear matrix inequalities (LMIs), as a method to ensure stability of  
145 linear dynamical systems. The methods also have applicability to non-linear systems,  
146 and several authors have used LMI analysis to learn non-linear dynamical systems by  
147 constraining the linearized systems to have global Lyapunov functions [21, 2, 55],

148 Even though the constraints

$$149 \quad Q \succeq I, \quad A^T Q + Q A + \alpha Q \preceq 0 \quad (1.8)$$

150 are convex in  $A$  and  $Q$  separately, they are not convex in  $A$  and  $Q$  jointly. Thus, the  
151 problem of jointly learning a stable linear dynamical system and its corresponding  
152 Lyapunov function, even for the simple linear-quadratic setting, is *not* a convex  
153 optimization problem, and alternative techniques such as alternating minimization  
154 need to be employed instead. Past work has considered different heuristics, such as  
155 approximately projecting a dynamics function  $A$  onto the (non-convex) stable set of  
156 matrices with eigenvalues  $\text{Re}(\lambda_i(A)) < 0$  [3]. It is no surprise, then, that learning  
157 stable non-linear systems is even more challenging:

158 **Stability of non-linear systems** For general non-linear systems, establishing  
159 stability via Lyapunov techniques is even more challenging. For the typical task here,  
160 which is that of establishing stability of some *known* dynamics  $\dot{x}(t) = f(x(t))$ , finding  
161 a suitable Lyapunov function is often more an art than a science. Although some  
162 general techniques such as sum-of-squares certification [43, 42] provide methods for  
163 certifying stability of polynomial (or similar) systems, these are often expensive and  
164 don't easily scale to high dimensional systems. Our proposed approach here is able  
165 to learn provably stable systems without solving this generally hard problem. While  
166 it is difficult to find a Lyapunov function that certifies the stability of some *known*  
167 system, we exploit the fact that it is relatively much easier to *enforce* some function  
168 to behave in a stable manner according to a Lyapunov function.

169 **Lyapunov functions in deep learning** Finally, there has been a small set of  
170 recent work exploring the intersection of deep learning and Lyapunov analysis [6,  
171 45, 51]. Although related to our work here, the approach in this past work is quite  
172 different. As is more common in the control setting, these papers try to learn neural-  
173 network-based Lyapunov functions for control policies, but in way that enforces  
174 stability via a loss penalty. For instance Richards et al., [45] optimize a loss function

175 that encourages  $\dot{V}(x) \leq 0$  for  $x$  in some training set. In contrast, our work guarantees  
 176 stability everywhere in the state space, not just at a small set of points; but only  
 177 for a simpler setting where the entire dynamics are to be learned (and hence can be  
 178 ‘constrained to be stable) rather than a stabilizing controller for known dynamics.

### 179 **1.3 Joint learning of dynamics and Lyapunov func-** 180 **tions**

181 The intuition of the approach we propose in this paper is straightforward: instead  
 182 of learning a dynamics function and attempting to separately verify its stability via  
 183 a Lyapunov function, we propose to jointly learn a dynamics model and Lyapunov  
 184 function, where the dynamics is inherently constrained to be stable (everywhere in  
 185 the state space) according to the Lyapunov function.

186 Specifically, following the principles mentioned above, let  $\hat{f} : \mathbb{R}^n \rightarrow \mathbb{R}^n$  denote a  
 187 “nominal” unconstrained dynamics model, and let  $V : \mathbb{R}^n \rightarrow \mathbb{R}$  be a positive definite  
 188 function:  $V(x) \geq 0$  for  $x \neq 0$  and  $V(0) = 0$ . Then in order to (provably, globally)  
 189 ensure that a dynamics function is stable, we can simply project  $\hat{f}$  such that it points  
 190 down the gradient of the Lyapunov function. This corresponds to the condition

$$191 \quad \nabla V(x)^T \hat{f}(x) \leq -\alpha V(x) \quad (1.9)$$

192 i.e., we define the dynamics

$$\begin{aligned}
 f(x) &= \text{Proj} \left( \hat{f}(x), \{f : \nabla V(x)^T f \leq -\alpha V(x)\} \right) \\
 &= \begin{cases} \hat{f}(x) & \text{if } \nabla V(x)^T \hat{f}(x) \leq -\alpha V(x) \\ \hat{f}(x) - \frac{\nabla V(x)}{\|\nabla V(x)\|_2^2} \left( \nabla V(x)^T \hat{f}(x) + \alpha V(x) \right) & \text{otherwise} \end{cases} \\
 &= \hat{f}(x) - \frac{\nabla V(x)}{\|\nabla V(x)\|_2^2} \text{ReLU}(\nabla V(x)^T \hat{f}(x) + \alpha V(x))
 \end{aligned}$$

193 (1.10)

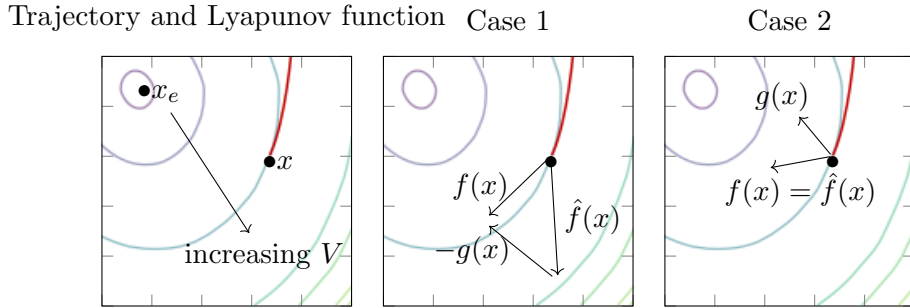


Figure 1.1: We plot the trajectory and the contour of a Lyapunov function of a stable dynamical system and illustrate our method. Let  $g(x) = \frac{\nabla V(x)}{\|\nabla V(x)\|_2} \text{ReLU}(\nabla V(x)^T \hat{f}(x) + \alpha V(x))$ . In the first case  $\hat{f}(x)$  has a component  $g(x)$  not in the half-space, which we subtract to obtain  $f(x)$ . In the second case  $\hat{f}(x)$  is already in the half-space, so is returned unchanged.

194 where  $\text{Proj}(x; \mathcal{C})$  denotes the orthogonal projection of  $x$  onto the point  $\mathcal{C}$ , and where  
 195 the second equation follows from the analytical projection of a point onto a half-space.  
 196 As long as  $V$  is defined using automatic differentiation tools, it is straightforward to  
 197 include the gradient  $\nabla V$  terms into the definition of  $f$ , and our final network can  
 198 be trained just like any other function. The general approach here is illustrated in  
 199 Figure 1.1.

### 200 1.3.1 Properties of the Lyapunov function $V$

201 Although the treatment above seems to make the problem of learning stable systems  
 202 quite straightforward, the subtlety of the approach lies in the choice of the function  
 203  $V$ . Specifically,  $V$  needs to be positive definite and needs to have no local optima  
 204 except the global optimum at 0. This is due to Lyapunov decrease condition: recall  
 205 that we are attempting to guarantee stability to the equilibrium point  $x = 0$ , yet  
 206 the decrease condition imposed upon the dynamics means that  $V$  is decreasing along  
 207 trajectories of  $f$ . If  $V$  has a local optimum away from the origin, the dynamics may  
 208 get stuck in this location; this manifests as the  $\|\nabla V(x)\|_2^2$  term going to zero.

209 To enforce these conditions, we make the following design decisions regarding  $V$ :

210 **No local optima.** We represent  $V$  via an input-convex neural network (ICNN)  
 211 function  $g : \mathbb{R}^n \rightarrow \mathbb{R}$  [1], which enforces the condition that  $g(x)$  be convex in its  
 212 inputs  $x$ . Such a network is given by the recurrence

$$\begin{aligned}
 z_1 &= \sigma_0(W_0x + b_0) \\
 z_{i+1} &= \sigma_i(U_i z_i + W_i x + b_i) \quad i \in \{1, \dots, k-1\}. \\
 g(x) &\equiv z_k
 \end{aligned}
 \tag{1.11}$$

214 For layer  $i+1$ :  $W_i$  are weights mapping from the input  $x$  to the  $i+1$  layer activations;  
 215  $U_i$  are positive weights mapping previously layer activations  $z_i$  to the next layer;  $b_i$   
 216 are real-valued biases; and  $\sigma_i$  are convex, monotonically non-decreasing non-linear  
 217 activations such as the ReLU or smooth variants. It is straightforward to show that  
 218 with this formulation,  $g$  is convex in  $x$  [1], and indeed any convex function can be  
 219 approximated by such networks [5].

220 **Positive definite.** The ICNN property enforces that  $V$  has only a single global  
 221 optimum; for  $V$  to be positive definite, we must also enforce that this optimum is  
 222 at  $x = 0$ . We could fix this by removing the bias term from Equation 1.11, but  
 223 this would mean we could no longer represent arbitrary convex functions. We could  
 224 also shift whatever global minimum to the origin, but that would require finding  
 225 finding the global minimum during training, which itself is computationally expensive.  
 226 Instead, we take an alternative approach: we shift the function such that  $V(0) = 0$ ,  
 227 and add a small quadratic regularization term to ensure strict positive definiteness.

$$V(x) = \sigma_{k+1}(g(x) - g(0)) + \epsilon \|x\|_2^2.
 \tag{1.12}$$

229 where  $\sigma_k$  is a positive convex non-decreasing function with  $\sigma_k(0) = 0$ ,  $g$  is the ICNN  
 230 defined previously, and  $\epsilon$  is a small constant. These terms together still enforce  
 231 (strong) convexity and positive definiteness of  $V$ .

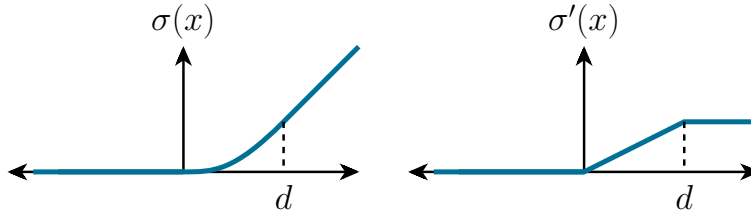


Figure 1.2: Rectified Huber Unit (ReHU), necessary for continuously differentiable Lyapunov functions.

232 **Continuously differentiable.** Although not always required, several of the condi-  
 233 tions for Lyapunov stability are simplified if  $V$  is continuously differentiable. ReLU  
 234 is discontinuous around 0, and the soft-plus smoothed ReLU is not zero at the origin.  
 235 We use a smoothed version with quadratic knee in  $[0, d]$ , called the Rectified Huber  
 236 Unit (ReHU):

$$237 \quad \sigma(x) = \begin{cases} 0 & \text{if } x \leq 0 \\ x^2/2d & \text{if } 0 < x < d. \\ x - d/2 & \text{otherwise} \end{cases} \quad (1.13)$$

238 An illustration of this activation is shown in Figure 1.2.

239 **Optionally warped input space.** Our construction so far guarantees that the  
 240 Lyapunov function has no local optima by making it convex. This is sufficient but not  
 241 necessary, and it may even impose too strict a constraint on the learned dynamics.  
 242 We can relax this function by allowing the input to the ICNN to be warped by any  
 243 continuously differentiable invertible function  $F : \mathbb{R}^n \times \mathbb{R}^n$ . i.e., using

$$244 \quad V(x) = \sigma_{k+1}(g(F(x)) - g(F(0))) + \epsilon \|x\|_2^2. \quad (1.14)$$

245 as the Lyapunov function. Invertibility ensures that the level sets of  $V$ , which are  
 246 convex, map to contiguous regions of the composite function  $g \circ F$ . This allows the  
 247 resultant Lyapunov function to be non-convex without having any optima other than  
 248 the global.

249 With these conditions in place, we have the following result.

250 **Theorem 1.** *The dynamics defined by*

$$251 \quad \dot{x} = f(x) \quad (1.15)$$

252 *are globally exponentially stable to the equilibrium point  $x = 0$ . Where  $f$  is from*  
 253 *Eqn. 1.10 and  $V$  is from Eqn. 1.12 or Eqn. 1.14, and  $\hat{f}$  and  $V$  functions have finite,*  
 254 *bounded weights.*

255 *Details.* The proof is straightforward, and relies on the properties of the networks  
 256 created above. First, note that by our definitions we have, for some  $M$ ,

$$257 \quad \epsilon \|x\|_2^2 \leq V(x) \leq M \|x\|_2^2 \quad (1.16)$$

258 where the lower bound follows from Eqn. 1.12 and the fact that  $g$  is positive. The  
 259 upper bound follows from the fact that the ReHU activation is linear for large  $x$  and  
 260 quadratic around 0. This in turn implies that  $V(x)$  behaves linearly as  $\|x\| \rightarrow \infty$ , and  
 261 is quadratic around the origin, so can be upper bounded by some quadratic  $M \|x\|_2^2$ .

262 The fact the  $V$  is continuously differentiable means that  $\nabla V(x)$  (in  $f$ ) is defined  
 263 everywhere, bounds on  $\|\nabla V(x)\|_2^2$  for all  $x$  follows from the Lipschitz property of  
 264  $V$ , the fact that  $0 \leq \sigma'(x) \leq 1$ , and the  $\epsilon \|x\|_2^2$  term

$$265 \quad \epsilon \|x\|_2 \leq \|\nabla V(x)\|_2 \leq \sum_{i=1}^k \prod_{j=i}^k \|U_j\|_2 \|W_i\|_2 \quad (1.17)$$

266 where  $\|\cdot\|_2$  denotes the operator norm when applied to a matrix. This implies that  
 267 the dynamics are defined and bounded everywhere owing to the choice of function  $\hat{f}$ .

268 Now, consider some initial state  $x(0)$ . The definition of  $f$  implies that

$$269 \quad \frac{d}{dt} V(x(t)) = \nabla V(x)^T \frac{d}{dt} x(t) = \nabla V(x)^T f(x) \leq -\alpha V(x(t)). \quad (1.18)$$

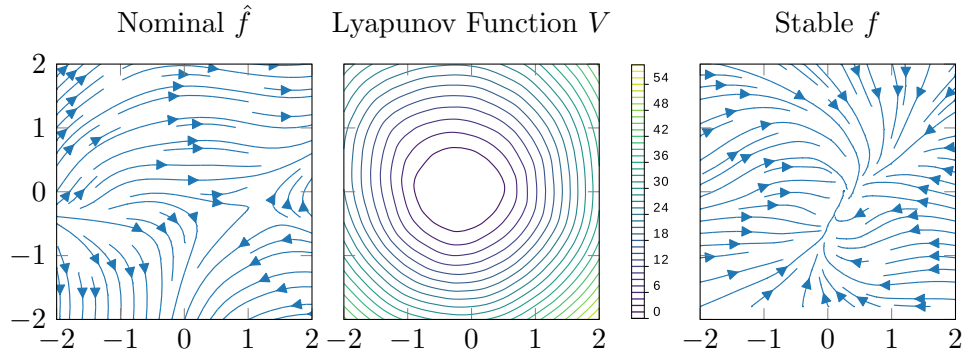


Figure 1.3: (left) Nominal dynamics  $\hat{f}$  for random network; (center) Convex positive definite Lyapunov function generated by random ICNN with constraints from Section 1.3.1; (right) Resulting stable dynamics  $f$ .

270 Integrating this equation gives the bound

$$271 \quad V(x(t)) \leq V(x(0))e^{-\alpha t} \quad (1.19)$$

272 and applying the lower and upper bounds gives

$$273 \quad \epsilon \|x(t)\|_2^2 \leq M \|x(0)\|_2^2 e^{-\alpha t} \implies \|x(t)\|_2 \leq \frac{M}{\epsilon} \|x(0)\|_2 e^{-\alpha t/2} \quad (1.20)$$

274 as required for global exponential convergence.  $\square$

## 275 1.4 Empirical results

276 We illustrate our technique on several example problems, first highlighting the inherent  
 277 stability of the method for random networks, demonstrating learning on simple  $n$ -  
 278 link pendulum dynamics, and finally learning high-dimensional stable latent space  
 279 dynamics for dynamic video textures via a VAE model.

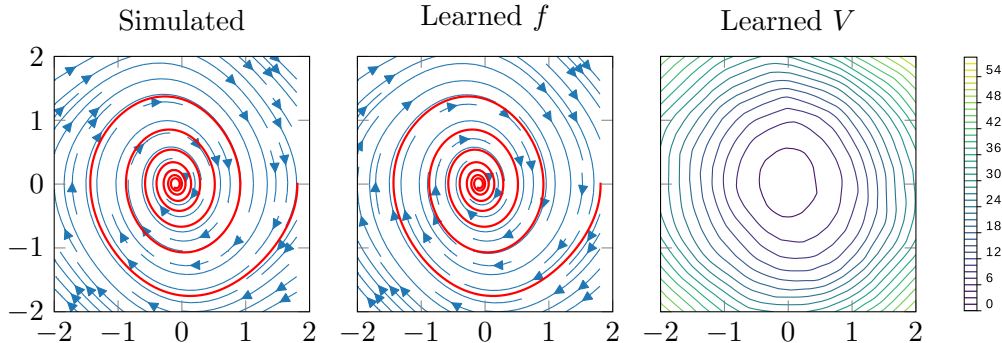


Figure 1.4: Dynamics of a simple damped pendulum. From left to right: the dynamics as simulated from first principles, the dynamics model  $f$  learned by our method, and the Lyapunov function  $V$  learned by our method (under which  $f$  is non-expansive).

### 280 1.4.1 Random networks

281 As a powerful visualization of the fact that our model is stable by construction, we  
 282 can plot the dynamics created by random networks, i.e., without any training at all.  
 283 Because the dynamics models are inherently stable, these random networks lead to  
 284 stable dynamics with interesting behaviors, illustrated in Figure 1.3. Specifically, we  
 285 let  $\hat{f}$  be defined by a fully connected network and  $V$  be an ICNN. Both networks have  
 286 two hidden layers with 100 nodes each, and are initialized by the Kaiming uniform  
 287 initialization [18]. The  $U$  weights in the ICNN are further subject to a softplus unit  
 288 to make them positive.

### 289 1.4.2 $n$ -link pendulum

290 Next we look at the ability of our approach to model a dynamical system from  
 291 kinematics, specifically the  $n$ -link pendulum. A damped, rigid  $n$ -link pendulum's  
 292 state  $x$  can be described by the angular position  $\theta_i$  and angular velocity  $\dot{\theta}_i$  of each  
 293 link  $i$ . As before  $\hat{f}$  and the Lyapunov function  $V$  have two hidden layers of 100 nodes,  
 294 with properties described in Section 1.3.1. Models are trained with pairs of data  
 295  $(x, \dot{x})$  produced by the symbolic algebra solver `sympy`, using simulation code adapted  
 296 from [56].

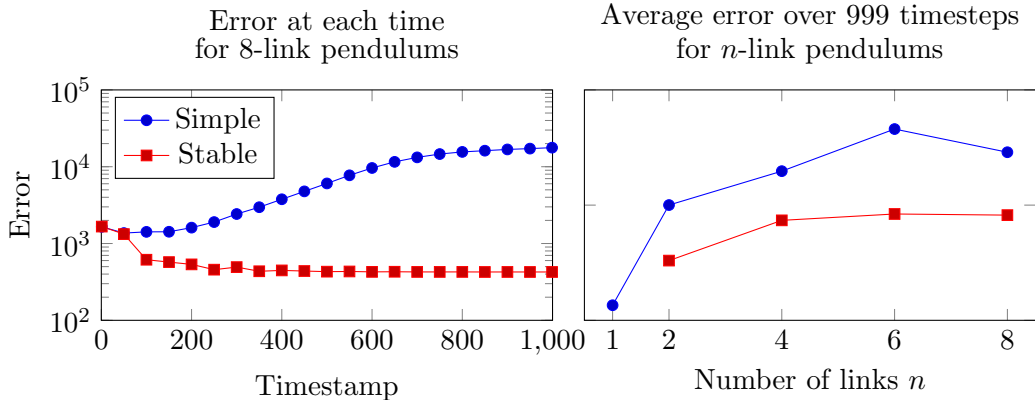


Figure 1.5: Error in predicting  $\theta, \dot{\theta}$  in 8-link pendulum at each timestep (left); and average error over 999 timesteps as the number of links in the pendulum increases (right).

297 In Figure 1.4, we compare the simulated dynamics with the learned dynamics in the  
 298 case of a simple damped pendulum (i.e. with  $n = 1$ ), showing both the vector field  
 299 and a single simulated trajectory, and draw a contour plot of the learned Lyapunov  
 300 function. As seen, the system is able to learn dynamics that can accurately predict  
 301 motion of the system even over long time periods. We can also recover the laws of  
 302 conservation of energy implicit in the data, including the fact that kinetic energy is  
 303 lost slowly but not potential energy.

304 We also evaluate the learned dynamics quantitatively varying  $n$  and the time horizon  
 305 of simulation. Figure 1.5 presents the total error over time for the 8-link pendulum,  
 306 and the average cumulative error over 1000 time steps for different values of  $n$ . While  
 307 both the simple and stable models show increasing mean error at the start of the  
 308 trajectory, our model is able to capture the loss of energy in the physical system and  
 309 in fact exhibits decreasing error towards the end of the simulation. In comparison,  
 310 the error in the simple model increases.

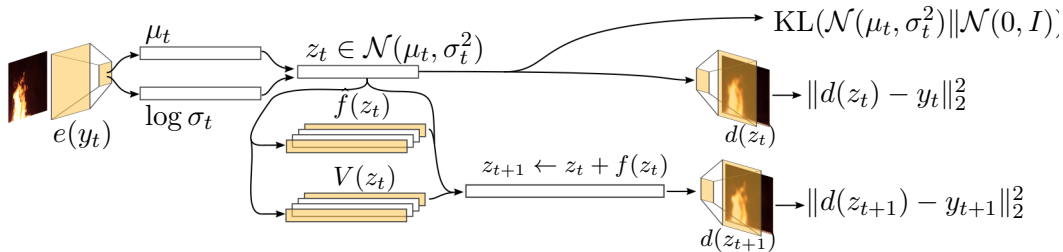


Figure 1.6: Structure of our video texture generation network. The encoder  $e$  and decoder  $d$  form a Variational Autoencoder, and the stable dynamics model  $f$  is trained together with the decoder to predict the next frame in the video texture.

### 311 1.4.3 Video Texture Generation

312 Finally, we apply our technique to stable video texture generation, using a Variational  
 313 Auto-Encoder (VAE) [23] to learn an encoding for images, and our stable network to  
 314 learn a dynamics model in the latent space. Given a sequence of frames  $(y_0, y_1, \dots)$ ,  
 315 we feed the network the frame at current time  $t$  and train it to reconstruct the frames  
 316 at the current time  $t$  and subsequent time-step  $t + 1$ . Specifically, we consider a  
 317 VAE defined by the encoder  $e : \mathcal{Y} \rightarrow \mathbb{R}^{2n}$  giving mean and variance  $\mu, \log \sigma_t^2 = e(y_t)$ ,  
 318 latent state  $z_t \in \mathbb{R}^n \sim \mathcal{N}(\mu_t, \sigma_t^2)$ , and decoder  $d : \mathbb{R}^n \rightarrow \mathcal{Y}$ ,  $y_t \approx d(z_t)$ . We train the  
 319 network to minimize both the standard VAE loss (reconstruction error plus a KL  
 320 divergence term), but *also* minimize the reconstruction loss of a next predicted state.  
 321 We model the evolution of the latent dynamics at  $z_{t+1} \approx f(z_t)$ , or more precisely  
 322  $y_{t+1} \approx d(f(z_t))$ . In other words, as illustrated in Figure 1.6, we train the full system  
 323 to minimize

$$\begin{aligned}
 324 \quad & \underset{e, d, \hat{f}, V}{\text{minimize}} \sum_{t=1}^{T-1} \left( \text{KL}(\mathcal{N}(\mu_t, \sigma_t^2 I) \parallel \mathcal{N}(0, I)) + \mathbf{E}_z [\|d(z_t) - y_t\|_2^2 + \|d(f(z_t)) - y_{t+1}\|_2^2] \right) \\
 & \hspace{20em} (1.21)
 \end{aligned}$$

325 We train the model on pairs of successive frames sampled from videos. To generate  
 326 video textures, we seed the dynamics model with the encoding of a single frame

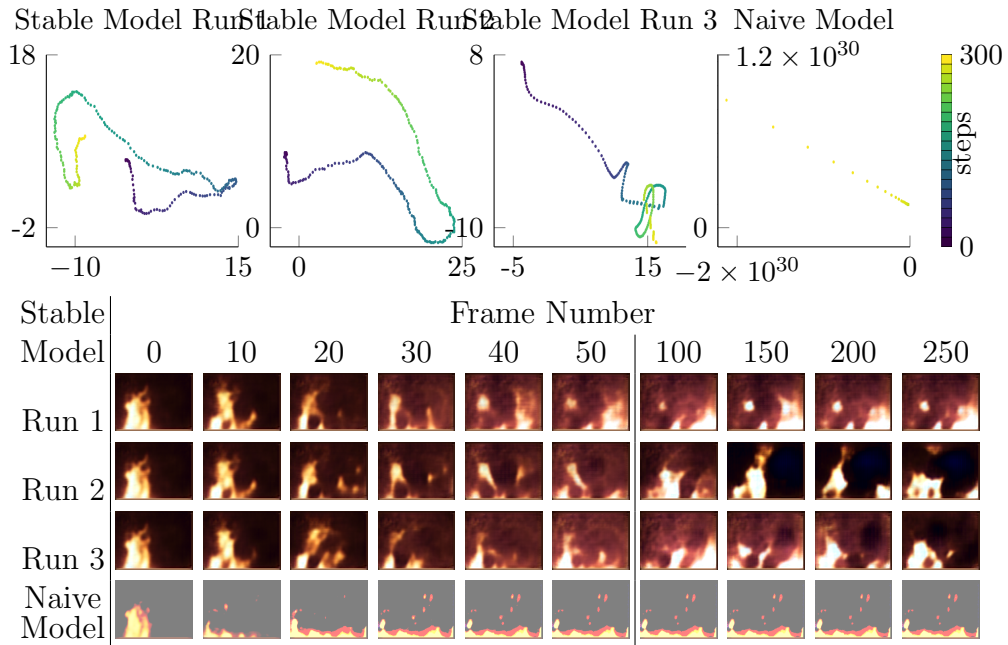


Figure 1.7: Samples generated by our stable video texture networks, with associated trajectories above. The true latent space is 320-dimensional; we project the trajectories onto a two-dimensional plane for display. For comparison, we present the video texture generated using an unconstrained neural network in place of our stable dynamics model.

327 and numerically integrate the dynamics model to obtain a trajectory. The VAE  
328 decoder converts each step of the trajectory into a frame. In Figure 1.7, we present  
329 sample stable trajectories and frames produced by our network. For comparison,  
330 we also include an example trajectory and resulting frames when the dynamics are  
331 modelled without the stability constraint (i.e. letting  $f$  in the above loss be a generic  
332 neural network). For the naive model, the dynamics quickly diverge and produce  
333 a static image, whereas for our approach, we are able to generate different (stable)  
334 trajectories that keep generating realistic images over long time horizons. We control  
335 the “temperature” of the generation process by adding controlled amounts of random  
336 noise to the system at each step.

## 337 1.5 Conclusion

338 We proposed a method for learning provably stable non-linear dynamical systems using  
339 neural networks. The approach jointly learns a convex positive definite Lyapunov  
340 function along with dynamics constrained to be stable according to these dynamics  
341 everywhere in the state space. We show that these models can be integrated into  
342 other deep architectures such as VAEs, and learn complex latent space dynamics  
343 is a fully end-to-end manner. Although we have focused here on the autonomous  
344 (i.e. uncontrolled) setting, the method opens several directions for future work, such  
345 as integration into dynamical systems for control or for model-based reinforcement  
346 learning settings. Having stable dynamics as a neural-network primitive can be useful  
347 in many diverse contexts, and combining these stable systems with the representational  
348 power of deep networks offers a powerful tool in modeling dynamical systems.

## 349 1.6 Adaptation to Stable Control and RL

350 After the successes of our stable dynamics model, we attempted to extend it to also  
351 learn stable policies and value functions. The intuitive extension to this is to replace  
352 the dynamics model  $\hat{f}$  with fixed (known) dynamics  $\tilde{f}$  and a learnable policy network

353  $\pi$ . That is, we train to minimize:

$$354 \quad \text{ReLU}(\nabla V(x)^T \tilde{f}(x, \pi) + \alpha V(x)) \quad (1.22)$$

355 given traces from simulated dynamics. We also transformed the dynamics so that  
356 the goal state was positioned at the origin, choosing suitable transformations for the  
357 dynamics and Lyapunov functions. As required by the approach, we attempted to  
358 train it from trajectory samples to minimize the error over one step.

359 We were able to successfully learn stabilizing controllers for toy examples such as a  
360 simple damped pendulum and for the cartpole problem. Unfortunately, we were not  
361 able to learn a swing-up controller for either environment, or any type of controller  
362 for an Acrobot<sup>2</sup> or more complex locomotion tasks. We observed that the training  
363 would consistently fail in the same way: the nominal dynamics function would diverge  
364 to the point of uselessness, followed by the learned Lyapunov function collapsing to a  
365 trivial function.

366 This persists despite any amount of regularization, hyperparameter tuning, and  
367 even across a variety of environments. Contemporary efforts in the literature were  
368 similarly unable to scale this approach to locomotion tasks. The consistent failure  
369 of this method suggested that an underlying principle was being violated, and that  
370 regularization was not able to address that. We eventually investigated how the  
371 difference in distributions between the data used to train the purportedly stable  
372 controller and the policy the controller was attempting to learn, which led us to the  
373 work in the next chapter.

<sup>2</sup>A two-link pendulum with a single actuator in the middle joint. A pendulum with an actuator at the fixed joint is a Pendubot [52].



## 374 Chapter 2

# 375 The Pitfalls of Regularization in 376 Off-Policy TD Learning

377 Temporal Difference (TD) learning is ubiquitous in reinforcement learning, where it is  
378 often combined with off-policy sampling and function approximation. Unfortunately,  
379 this combination of conditions (the *deadly triad*) often leads to unstable training and  
380 unbounded error. Modern RL methods often implicitly assume that regularization is  
381 sufficient to mitigate the problem and the standard deadly triad examples from the  
382 literature are not able to refute this. In this chapter, we introduce a series of new  
383 counterexamples to show that this problem is not solved by regularization. We show  
384 that TD methods can fail to learn a non-trivial value function under *any* amount of  
385 regularization, that regularization can itself induce divergence; and we show that one  
386 of the most promising mitigations (Emphatic-TD algorithms) may also diverge under  
387 regularization. We further demonstrate such divergence when using neural networks  
388 as function approximators. Thus, we argue that there needs to be much more care in  
389 the application of regularization to RL methods.

390 *From “The Pitfalls of Regularization in Off-Policy TD Learning” by Manek and*  
391 *Kolter (2022)*

## 392 2.1 Introduction

393 Temporal Difference (TD) learning is a method for learning expected future-discounted  
394 quantities from Markov processes, using transition samples to iteratively improve  
395 estimates. This is most commonly used to estimate expected future-discounted  
396 rewards (the *value function*) in Reinforcement Learning (RL). Advances in RL allow  
397 us to use powerful function approximators, and also to use “off-policy” sampling  
398 strategies (i.e. which do not naively follow the underlying Markov process.) When TD,  
399 function approximation, and off-policy training are all combined, learned functions  
400 exhibit severe instability and divergence, as classically observed by Williams and  
401 Baird III [59] and Tsitsiklis and Van Roy [54]. This combination is known in the  
402 literature as the *deadly triad* [48, pg. 264], and while many contemporary variants  
403 of TD are designed to converge despite the instability, the quality of the solution at  
404 convergence may be arbitrarily poor [24].

405 A common technique to avoid unbounded error is  $\ell_2$  *regularization* [53], i.e. penalizing  
406 the squared norm of the weights in addition to the TD error. This is generally  
407 understood to bound the worst-case error in exchange for biasing the model and  
408 potentially increasing the error everywhere else. When used on three common  
409 examples of the deadly triad [24, 59, 48, pg. 260], regularization appears to mitigate  
410 the worst aspects of the divergence in practice. Consequently, it has become an  
411 essential assumption made by many RL algorithms [8, 33, 50, 61, 64, 63, 27] and is  
412 seen as routine and innocuous.

413 We argue that this perspective on regularization in off-policy TD is fundamentally  
414 mistaken. While regularization is indeed well-behaved and innocuous in classic  
415 fully-supervised contexts, the use of bootstrapping in TD means that even small  
416 amounts of model bias induced by regularization can cause divergence. This is  
417 an oft-ignored phenomenon in the literature, and so we introduce a series of new  
418 counterexamples (summarized in Table 2.1) to show how regularization can have  
419 counterintuitive and destructive effects in TD. We show that vacuous solutions  
420 and training instability are *not* solved by the use of regularization; that applying

421 regularization can sometimes induce divergence and increase worst-case error; and  
422 that Emphatic-TD based algorithms—which are the most promising way to correct  
423 stability from off-policy training—can themselves diverge when regularized. We  
424 finally also illustrate misbehaving regularization in the context of neural network  
425 value function approximation, demonstrating the general pitfalls of regularization  
426 possible in RL algorithms. Regularization needs to be treated cautiously in the  
427 context of RL, as it behaves differently than in supervised settings.

428 Our counterexamples demonstrate these core ideas:

429 **TD learning off-policy can be unstable and/or have unbounded error even**  
430 **when it converges.** Following well-established methods we show there is some  
431 off-policy distribution under which TD with linear value function approximation  
432 diverges *and* learns a model with unbounded error (even if it were able to converge  
433 to the TD fixed point). This concisely demonstrates key features of the training  
434 error: the error is small when the distribution is close to on-policy, but the error  
435 diverges around specific off-policy distributions. The intuition behind this, explained  
436 in Section 2.3, is that the off-policy<sup>1</sup> TD update involves a projection operation that  
437 depends on the sampling distribution and can be arbitrarily far away from the true  
438 value. This basic fact has already been established by past work [59, 24], but our  
439 example is based upon a particular simple three-state MP, drawn in Figure 2.1a.

440 **Regularization cannot always mitigate off-policy training error.** We next  
441 introduce regularization into our setting, and show how it changes the relationship  
442 between training error and off-policy training. As explained in Section 2.2, we penalize  
443 the  $\ell_2$ -norm of learned (linear) weights with some coefficient  $\eta$ ; as  $\eta$  increases, the  
444 learned weights approach zero. However, in **Example 1**, we show that there exists  
445 an off-policy distribution such that for any non-negative  $\eta$ , the regularized TD fixed  
446 point attains strictly higher approximation error than the zero solution (i.e., the  
447 infinitely regularized point). We call such examples *vacuous*. In other words, vacuous

<sup>1</sup>We consider a sampling distribution to be *on-policy* if it follows the stationary distribution of the MP and *off-policy* otherwise; we do not explicitly consider a separate policy in this chapter.

448 value functions never do better than guessing zero for all states, for any amount of  
449 regularization.

450 We further analyze this vacuous example in the context of the algorithm in [63].  
451 In this work, the authors assume the use of regularization to derive bounds on the  
452 learned error under off-policy sampling. Although these bounds are technically correct  
453 in the case of our counterexample, they are very loose, at about 2000 times the limit  
454 of vacuity. This highlights the challenge of formally relying on regularization to bound  
455 model error, and illustrates the danger of relying on regularization in theoretical RL.

456 **Small amounts of regularization can cause model divergence.** There is a  
457 general implicit assumption in much ML literature that regularization monotonically  
458 shrinks learned weights and consequently the model output. This intuition comes  
459 from classic fully-supervised machine learning where it typically holds. But because  
460 TD bootstraps value estimates (i.e. learns values using its own output), the regularizer  
461 is composed arbitrarily often, and so it is possible for small amounts of bias to be  
462 arbitrarily magnified. We dub this phenomenon “small-eta divergence” and illustrate  
463 it in **Example 2**. We relate this to the presence of negative eigenvalues in an  
464 intermediate step of the solution and show that, in some settings, the error of the  
465 TD solution may be relatively small when applied with no regularization but adding  
466 regularization causes the model to have *worse* error than the zero solution.

467 One common solution to this problem is to lower-bound  $\eta$  to guarantee that regular-  
468 ization behaves monotonically. However, we further show that such a lower bound  
469 may restrict the model to a domain in which the model is vacuous. That is, a model  
470 that is not vacuous becomes vacuous when regularized with this lower bound. We  
471 also show that it is not always possible to select a single  $\eta$  *a priori*, with examples  
472 of mutually-incompatible off-policy distributions where there is no  $\eta$  that achieves  
473 better than vacuous or nearly-vacuous results at different distributions.

474 **Emphatic-TD-based algorithms are vulnerable to instability from regular-**  
475 **ization.** Emphatic-TD [49] attempts to solve the problem of training off-policy

476 by resampling TD updates so they appear to be on-policy. This technique requires  
 477 an emphasis model that decides how to scale each TD update, and learning this  
 478 has been the key challenge preventing widespread adoption of Emphatic-TD. A  
 479 recent paper [64] proposed learning this emphasis model using “reversed” TD while  
 480 simultaneously learning the value model using regular TD. The resultant algorithm  
 481 is called COF-PAC, and employs regularization to ensure that the two TD models  
 482 eventually converge.

483 We show that regularization, while necessary, can be harmful for such models in  
 484 **Example 3**. Specifically, we construct a model that converges to the correct solution  
 485 without regularization but to an arbitrarily poor solution when regularized. The  
 486 intuition behind this is that regularizing the emphasis model changes the effective  
 487 distribution of the TD updates to the value model, which can cause the value model  
 488 to have arbitrarily large error. We complete the example by showing that regularizing  
 489 the value function separately does not restore performance.

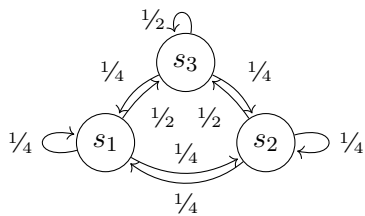
490 **Regularization can cause model divergence in neural networks.** So far  
 491 most analysis of the deadly triad in the literature focuses on the linear case. We  
 492 extend our example to a nine-state Markov chain (shown in Figure 2.8), and show how  
 493 the previously identified problems persist into the neural network case in **Example 4**.  
 494 We show two key similarities: first, models trained at certain off-policy distributions  
 495 may be vacuous. Second, small amounts of regularization counterintuitively *increase*  
 496 error. This illustrates Example 2 in the NN case.

## 497 2.2 Preliminaries and Notation

498 Consider the  $n$ -state Markov chain  $(\mathcal{S}, P, R, \gamma)$ , with state space  $\mathcal{S}$ , state-dependent  
 499 reward  $R : \mathcal{S} \rightarrow \mathbb{R}$ , and discount factor  $\gamma \in [0, 1]$ .  $P \in \mathbb{R}^{n \times n}$  is the transition matrix,  
 500 with  $P_{ij}$  encoding the probability of moving from state  $i$  to  $j$ . We wish to estimate  
 501 the value function  $V : \mathcal{S} \rightarrow \mathbb{R}$ , defined as the expected discounted future reward of  
 502 being in each state:  $V(s) \doteq \mathbf{E} [\sum_{t=0}^{\infty} \gamma^t R(s_t) | s_0 = s]$ . A key property is that it follows

- 
- 
- Example 1** There exist off-policy distributions under which TD learns a *vacuous* model (one which—despite any amount of regularization—never does better than guessing zeros).
- Example 2** Small values of the regularization parameter  $\eta$  can make TD diverge in models that otherwise converge. This is an unavoidable effect of bootstrapping in TD, and setting a lower-bound to exclude this may render models vacuous.
- Example 3** Emphatic-TD-inspired algorithms are a promising way to reweigh samples and mitigate the effects of training off-policy. However, if this reweighing is learned using TD, then regularization can bias the emphasis model and cause the value model itself to diverge.
- Example 4** Training instability and increased error due to the deadly triad also occur when neural networks are used. We construct an empirical example and draw qualitative comparisons.
- 
- 

Table 2.1: Summary of theorems.



(a) Three-state MP.

$$\frac{1}{4} \begin{bmatrix} 1 & 1 & 2 \\ 1 & 1 & 2 \\ 1 & 1 & 2 \end{bmatrix} \quad (2.1)$$

(b) Three-state MP.

Figure 2.1: Our three-state counterexample Markov Process. We use this to illustrate how TD models can fail despite common mitigating strategies with linear function approximation.

503 the Bellman equation:

$$504 \quad V = R + \gamma PV \quad (2.2)$$

Using linear function approximation to learn  $V$ , we assume a matrix of feature-vectors  $\Phi \in \mathbb{R}^{n \times k}$  that is fixed, and a vector of parameters  $w \in \mathbb{R}^k$  that is learned. The  
505 Bellman equation is then:

$$506 \quad \Phi w = R + \gamma P \Phi w \quad (2.3)$$

When  $w$  is learned with TD, this equation is only valid if the TD updates are *on-policy* (that is, they are distributed according to the steady-state probability of visiting each state, written as  $\pi \in \mathbb{R}^n$ ). In the general case, where TD updates follow a (possibly) different distribution  $\mu \in \mathbb{R}_0^n$ , the TD solution is a fixed point of the Bellman operator  
507 followed by a projection [24]:

$$508 \quad \Phi w = \Pi_\mu (R + \gamma P \Phi w) \quad (2.4)$$

where the matrix  $\Pi_\mu = \Phi(\Phi^\top D \Phi)^{-1} \Phi^\top D$  projects the Bellman backup onto the column-space of  $\Phi$ , reweighted by the state-distribution matrix  $D = \text{diag}(\mu)$ . This  
509 yields the closed-form solution:

$$510 \quad w = A^{-1} \vec{b} \quad (2.5)$$

511 Where  $A = \Phi^\top D (I - \gamma P) \Phi$  and  $\vec{b} = \Phi^\top D R$ . When this solution is subject to  $\ell_2$   
512 regularization, some non-negative  $\eta$  is added to ensure the matrix being inverted is  
513 positive definite:

$$514 \quad w^*(\eta) = (A + \eta I)^{-1} \vec{b} \quad (2.6)$$

515 As will be important later, we note that as  $\eta$  increases it drives  $w^*(\eta)$  towards zero.

## 516 2.3 Our Counterexamples

517 Under deadly triad conditions are present, TD may learn a value function with  
 518 arbitrarily large error even if the true value function can be represented with low  
 519 error. Consider the three-state MP in Figure 2.1a, which we instantiate with the  
 520 value function  $V = [1, 2.2, 1.05]^\top$  and discount factor  $\gamma = 0.99$ . The reward function  
 521 is computed as  $R \leftarrow (I - \gamma P)V$ . We choose a basis  $\Phi$  with small representation error  
 522  $\|\Pi_\mu V - V\| \leq \epsilon$ :

$$523 \quad \Phi = \begin{bmatrix} 1 & 0 \\ 0 & -2.2 \\ 1/2(1.05 + \epsilon) & -1/2(1.05 + \epsilon) \end{bmatrix} \quad \text{where } \epsilon > 0 \quad (2.7)$$

524 We first consider the unregularized ( $\eta = 0$ ) case, closely following the derivation  
 525 in [24]. We wish to show there is some sampling distribution  $\mu$  such that error in the  
 526 learned value function is unbounded. To do this, we set  $\mu = [0.56(1 - p), 0.56p, 0.44]$ ,  
 527 where  $p \in (0, 1)$ . We set  $\epsilon = 10^{-4}$  and find  $p$  around which  $A$  is ill-conditioned by  
 528 solving  $\det(A) = 0$ :

$$529 \quad p = 0.102631 \quad \vee \quad p = 0.807255 \quad (2.8)$$

530  $A^{-1}$  (and consequently the TD error) can be made arbitrarily large by selecting  $p$   
 531 close to these values, which completes the introductory example. Now we look at the  
 532 behavior of TD under regularization, which is the main contribution of this chapter.

### 533 2.3.1 Regularization cannot always mitigate the error from 534 training off-policy.

535 There is a belief in the literature that regularization is a trade-off between reducing  
 536 the blow-up of asymptotic errors and accurately learning the value function every-  
 537 where else [8, 63]. However, this belief does not accurately capture the nature of  
 538 regularization: we show that it is possible to learn models that never perform better

539 than always guessing zero despite any amount of regularization. That is, the TD  
 540 error at all  $\eta$  is at least as much as the error as  $\eta \rightarrow \infty$ . We call such models *vacuous*.

541 **Example 1.** We use the same setting as in Section 2.3. When TD is regularized,  
 542 there may exist some off-policy distribution at which TD learns a vacuous model. In  
 543 notation:

$$544 \quad \|\Phi w^*(\eta) - V\| \geq \lim_{\eta \rightarrow \infty} \|\Phi w^*(\eta) - V\| = \|\Phi \vec{0} - V\| = \|V\| \quad \forall \eta \in \mathbb{R}_0^+ \quad (2.9)$$

545 *Details.* We use the same setting as in Section 2.3. We observe that  $\hat{w} = [1, -1]^\top$   
 546 minimizes the least-squares error  $\|\Phi \hat{w} - V\|$ , and further observe that a sufficient  
 547 condition for a solution to be vacuous is that  $\hat{w}^\top w^*(\eta) \leq 0$ . Solving:

$$548 \quad 0 = \hat{w}^\top w^*(\eta) = \frac{\eta p - 0.233\eta - 0.304p^2 + 0.276p - 0.025}{\eta^2 + 1.44\eta p + 0.215\eta - 0.193p^2 + 0.175p - 0.016} \quad (2.10)$$

$$549 \quad \implies p \in \{0.102636, \dots\} \quad (2.11)$$

550 We verify that TD is vacuous at  $p = 0.102636$  by computing the TD error at  
 551 convergence:

$$552 \quad \|\Phi w^*(\eta) - V\|^2|_{p=\bar{p}} = \frac{\eta^2(0.148 + 0.744\eta + \eta^2)}{\eta^2(0.132 + 0.727\eta + \eta^2)} \|V\|^2 \geq \|V\|^2 \quad (\forall \eta \in \mathbb{R}^+) \quad (2.12)$$

553 Since the fraction term in Equation 2.12 is obviously improper, we can conclude  
 554 that our example will always have at least  $\|V\|$  error over all  $\eta$ , and is therefore  
 555 vacuous.  $\square$

556 We note that the error is not defined at  $\eta = 0$  because this corresponds to a model  
 557 divergence similar to our introductory example. In practice, the TD fixed point will  
 558 still converge to a vacuous solution:

$$559 \quad \lim_{\eta \rightarrow 0} \|\Phi w^*(\eta) - V\|^2 = \frac{0.148}{0.132} \|V\|^2 > \|V\|^2 \quad (2.13)$$

560 **Geometry of vacuous linear models.**

561 We begin by noting that we can easily find the solution  $\hat{w}$  that minimizes the least-  
562 squares error  $\|\Phi\hat{w} - V\|$ . If we consider this solution as a vector (as drawn in  
563 Figure 2.2a), we can immediately see that there is an  $\ell_2$ -ball around  $\hat{w}$  corresponding  
564 to the set of  $w^*(\eta)$  with no more than  $\|V\|$  error.

565 Similarly, we can trace the trajectory that the TD solution  $w^*(\eta)$  takes as  $\eta$  is  
566 increased from 0 to  $\infty$ . We know that, as  $\eta \rightarrow \infty$ ,  $w^*(\eta)$  is crushed to zero and so  
567 all trajectories must eventually terminate at the origin. When regularized models  
568 are not vacuous, the trajectory intersects the non-vacuous-error ball. We see this in  
569 trajectory 2, where the error briefly dips below  $\|V\|$  in Figure 2.2b.

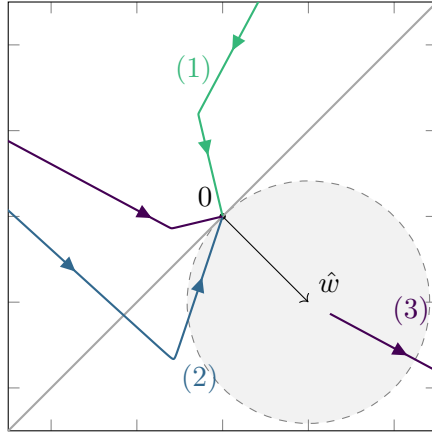
570 Intuitively, a sufficient condition for a solution to be vacuous is that it remains in the  
571 half-space that is tangent to and excludes the non-vacuous parameter ball. This is  
572 equivalent to finding some distribution  $\mu$  such that  $\hat{w}^\top w^*(\eta) \leq 0$  for all  $\eta$ , which we  
573 numerically solve to obtain the model in trajectory 1. From Figure 2.2a we can see  
574 the trajectory remains in the half-space, and from Figure 2.2b we can see that the  
575 error is never less than  $\|V\|$ . Trajectory 1 is a vacuous example.

576 We observe that Example 1, because it remains entirely in the half-space  $\hat{w}^\top w^*(\eta) \leq 0$ ,  
577 could easily be generalized to any form of convex regularization such as  $\ell_1, \ell_2, \ell_\infty$ , etc.  
578 We leave this for future work.

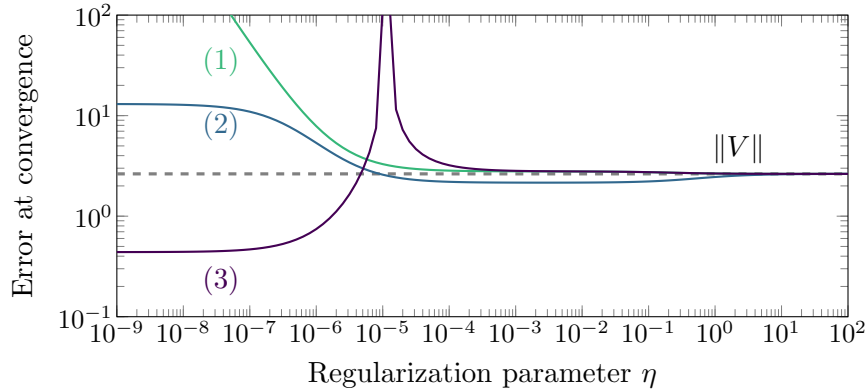
579 This intuition does not persist in the neural network case (discussed in Section 2.3.4).  
580 In that case, the relationship between parameters and error does not admit a clean  
581 non-vacuous ball, but instead a deeply non-linear set of states. The resultant geometry  
582 does not admit a clean, intuitive, explanation.

583 **A second example.**

584 We present a second example where the error is stationary with respect to the  
585 regularization parameter. This is worse than Example 1 because we are able to show  
586 that the point the model converges to is *independent* of regularization. This example



(a) As  $\eta$  increases,  $w^*(\eta)$  traces different trajectories at different  $\mu$ .  $\hat{w}$  minimizes the error, and we shade the area with TD error less than  $\|V\|$ .



(b) We plot the error curves corresponding to the three  $w^*(\eta)$  trajectories, along with  $\|V\|$ . Trajectory 1 is vacuous because the error is at least  $\|V\|$  for all  $\eta$ .

Figure 2.2: Plotting the trajectory of the parameters on above and the errors below, we show how our counterexample 1 is never better than  $\|V\|$  because it remains in half-space where  $\hat{w}^\top w^*(\eta) \leq 0$ . For comparison, we show trajectory 2 that is improved by regularization, and 3, which exhibits small- $\eta$  errors. (The trajectories are distorted, so the errors in the two plots are not directly comparable.)

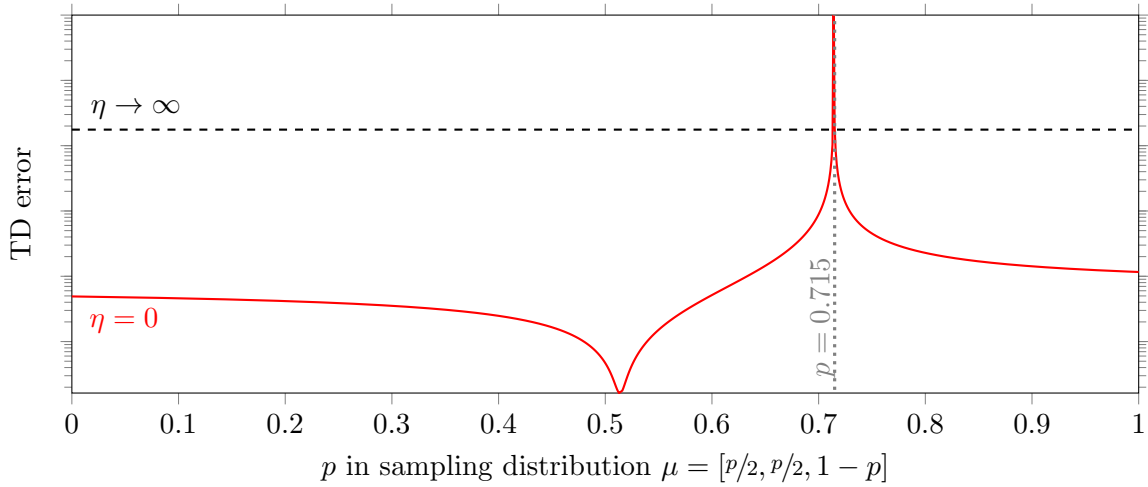


Figure 2.3: We plot TD error against  $p$  for our three-state MP with  $\epsilon = 10^{-4}$ . This shape is similar to that in [24]. There is a minima close to  $\pi$  ( $p \approx 0.5$ ), and an asymptote at the singularity ( $p \approx 0.715$ ). At different levels of regularization the error function moves between the unregularized case ( $\eta = 0$ ) and the limiting case ( $\eta \rightarrow \infty$ ), as analyzed in Section 2.3.1. We show that there is some  $p$  at which the error is never below the  $\eta \rightarrow \infty$  line.

587 is the natural three-state extension to the two-state counterexample by Kolter [24].

588 *Details.* We use the same setting as in Section 2.3, except the value function is  $V =$   
 589  $[1, 1, 1.05]^\top$  and basis  $\Phi$  selected to have small representation error  $\|\Pi_D V - V\| \leq \epsilon$ :

$$590 \quad \Phi = \begin{bmatrix} 1 & 0 \\ 0 & -1 \\ 1/2(1.05 + \epsilon) & -1/2(1.05 + \epsilon) \end{bmatrix} \quad \text{where } \epsilon > 0 \quad (2.14)$$

591 We set  $\epsilon = 10^{-4}$  and write down  $w^*(\eta)$  in terms of  $g$ , a scalar function of  $\eta$  and  $p$ :

$$592 \quad w^*(\eta) = (A + \eta I)^{-1} \vec{b} = \frac{(2\eta + p)(0.925 - 1.29p)}{100\eta^2 + 47.4p\eta + 1.85\eta - 1.30p^2 + 0.927p} \cdot \begin{bmatrix} 1 \\ -1 \end{bmatrix} \quad (2.15)$$

$$593 \quad \equiv g(p, \eta) \begin{bmatrix} 1 \\ -1 \end{bmatrix} \quad (2.16)$$

594 When  $g(p, \eta) \leq 0$ , the TD solution is vacuous. We show that directly:

$$595 \quad \|\Phi w^*(\eta) - V\| = \|g(p, \eta) \Phi * [1, -1]^\top - \Phi * [1, -1]^\top\| = \|g(\eta) - 1\| \cdot \|V\| \quad (2.17)$$

596 When  $g(p, \eta) \leq 0$ , then  $\|g(p, \eta) - 1\| \geq 1$  for all  $\eta$  and the TD solution is vacuous.  
 597 We find such a solution by noting the numerator has two roots in  $p$ , one of which  
 598 corresponds to a vacuous solution:  $g(0.715083, \eta) = 0$  ( $\forall \eta$ ), and this completes the  
 599 example!

600 In this setting, when TD updates follow the sampling distribution  $p \approx 0.715083$ , the  
 601 error of the model at convergence is always  $\|V\|$  regardless of regularization. Our  
 602 example converges to the same vacuous value regardless  $\eta$ .  $\square$

603 We present this graphically in Figure 2.3, where we plot the relationship between the  
 604 off-policy distribution and the error at the TD fixed point. We plot the error with no  
 605 regularization ( $\eta = 0$ ) and the limiting error ( $\eta \rightarrow \infty$ ).

606 We can see that the TD error intersects the  $\eta \rightarrow \infty$  line immediately before and after

607 the singularity. Our counterexample corresponds to the second root (that is, the  
 608 intersection point at higher  $p$ .) That corresponds to the stationary point between the  
 609 asymptote that is crushed and the error on the right that increases. If our simpler  
 610 derivation proved unsatisfying, we can also derive this counterexample using this fact:

$$611 \quad 0 = \frac{d}{d\eta} \hat{w}^\top w^*(\eta) = \frac{p(p - 0.715083)}{p(p - 0.714303)^2} \quad (2.18)$$

612 From this, we can easily see that the counterexample is at  $p = 0.715083$ . And this  
 613 completes the example! We have discovered some  $p$  at which the TD error is always  
 614 at least  $\|V\|$ , regardless of regularization, and so our example learns a vacuous value  
 615 function.

616 ***Breaking the Deadly Triad and our counterexample.***

617 In light of our example we examine the work of [63] in which the authors derive a  
 618 bound for the regularized TD error under a novel double-projection update rule. We  
 619 apply our example to their bound and show that their method may produce loose  
 620 bounds on TD solutions, and so doesn't quite break the deadly triad:

$$621 \quad \|\Phi w^*(\eta) - V\| \leq \frac{1}{\xi} \left( \frac{\sigma_{\max}(\Phi)^2}{\sigma_{\min}(\Phi)^4 \sigma_{\min}(D)^{2.5}} \cdot \|V\| \eta + \|\Pi_D V - V\| \right) \quad (2.19)$$

for  $\xi \in [0, 1]$ , where  $\sigma_{\max}$  and  $\sigma_{\min}$  denote the largest and smallest singular value  
 622 respectively. Theorem 2 from [63] bounds  $\eta$ , and therefore also  $b$ :

$$623 \quad \eta > \arg \inf_{\eta} \|\Phi - C_0\| = 0.177/(1 - \xi)^2 \quad (2.20)$$

$$624 \quad \inf_{\xi} b(\xi, \eta) = 5.20 \times 10^4 \approx 2000 * \|V\| \quad (2.21)$$

625 Their method bounds the error in our example by  $2000 * \|V\|$ , which is tremendously  
 626 loose.

627 Analyzing the second example starting from Equation 2.19:

$$628 \quad \|\Phi w^*(\eta) - V\| \leq b(\eta, \xi) = \frac{1}{\xi} \left( \frac{\sigma_{\max}(\Phi)^2}{\sigma_{\min}(\Phi)^4 \sigma_{\min}(D)^{2.5}} \cdot \|V\| \eta + \|\Pi_D V - V\| \right) \quad (2.22)$$

$$629 \quad = 1/\xi \cdot (38.0\eta + 8.07 \times 10^{-5}) \quad (2.23)$$

for  $\xi \in [0, 1]$ , where  $\sigma_{\max}$  and  $\sigma_{\min}$  denote the largest and smallest singular value  
630 respectively. Theorem 2 from [63] bounds  $\eta$ , and therefore also  $b$ :

$$631 \quad \eta > \arg \inf_{\eta} \|\Phi - C_0\| = 0.367(6.86 - 13.7\xi + 6.86\xi^2)^{-1} \quad (2.24)$$

$$632 \quad \inf_{\xi} b(\xi, \eta) = 13.8 = 7.86 * \|V\| \quad (2.25)$$

633 Under our example, their method bounds the error at no more than  $7.86 * \|V\|$ , which  
634 is a very loose bound that permits vacuous solutions. This illustrates the risk of  
635 trying to regularize away singularities, particularly in theoretical work.

636 Investigating the cause of the loose bounds reveals that the presence of  $\sigma_{\min}(D)^{2.5}$   
637 in 2.19 is largely responsible. As  $D$  is a diagonal matrix encoding the sampling  
638 distribution,  $\sigma_{\min}(D)$  is the smallest sampling rate of any state, and so the bound  
639 must be at least  $\frac{\eta}{\xi n^{2.5}}$  for any perfectly representable  $n$ -state MP. Unfortunately, this  
640 appears to be fundamental limit caused by finding a linear bound to an error that  
641 scales non-linearly, and following their derivation does not readily admit a way to  
642 improve this.

### 643 **2.3.2 Small amounts of regularization can cause large in-** 644 **creases in training error.**

645 There is a general assumption in the literature that  $\ell_2$  regularization monotonically  
646 shrinks the learned weights. While this is true in classification, regression, and other  
647 non-bootstrapping contexts, this is not true in TD. Because TD bootstraps values, it  
648 composes the regularization over itself arbitrarily deep, and so model bias may be  
649 arbitrarily magnified.

650 This can be understood in terms of the eigenvalues of the matrix  $A$  in Equation 2.6.  
 651 By increasing values along the diagonal,  $\ell_2$  regularization increases eigenvalues of  
 652 the matrix  $(A + \eta I)$  to ensure it is positive definite. Under off-policy distributions,  
 653 it is possible for  $A$  to have eigenvalues that are negative or zero. This implies that  
 654 there are  $\eta$  for which  $\det(A + \eta I) = 0$ , and selecting  $\eta$  close to these values allows us  
 655 to achieve arbitrarily high error. We show one such case in Example 2. This is not  
 656 merely theoretical—we demonstrate this in the neural network case in Section 2.3.4.

657 **Example 2.** When TD is regularized, the model may diverge around (typically  
 658 small) values of  $\eta$ . Lower-bounding  $\eta$ , a common mitigation, can make well-behaved  
 659 models vacuous. It is not always possible to select a single value of  $\eta$  that makes  
 660 models vacuous at different sampling distributions.

661 *Details.* Using our three-state example, we set  $\mu = [0.05, 0.05, 0.9]$  and solve for  
 662  $\det(A + \eta I) = 0$ :

$$663 \quad 0 = \det(A + \eta I) = \eta^2 + 5.45 \times 10^{-2} \eta - 7.47 \times 10^{-3} \quad \implies \quad \eta = 0.0634 \quad (2.26)$$

664 As in the introductory example, the error grows arbitrarily large as  $\eta \rightarrow 0.0634$ .  $\square$

665 The same analysis is repeated for our second example in 2.3.1. We set  $p = 0.9$  and  
 666 solve for  $\det(A + \eta I) = 0$ :

*Details.*

$$667 \quad 0 = 100\eta^2 + 47.4p\eta + 1.85\eta - 1.30p^2 + 0.927p \quad (2.27)$$

$$668 \quad \eta = 0.00482577 \quad \vee \quad \eta = -0.45 \quad (2.28)$$

669 Note that the denominator of  $g(p, \eta)$  is proportional to  $\det(A + \eta I)$ , and so  $g(0.9, \eta)$   
 670 and the error at the TD fixed point can be made arbitrarily large by selecting  $\eta$  close  
 671 to  $4.83 \times 10^{-3}$ . As this is the only positive root, the model does not diverge at other  
 672 values.  $\square$

673 This small- $\eta$  divergence effect can appear in several ways, illustrated in Figure 2.4a.

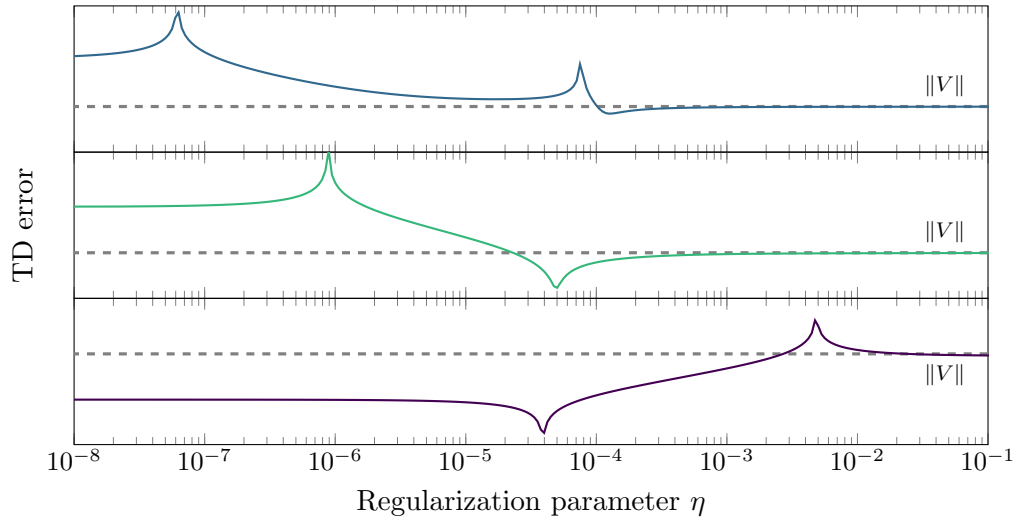
674 Typically, this appears as one or more points at which TD error diverges before the  
675 region at which regularization reduces the model error below  $\|V\|$ . The first and  
676 second plot in Figure 2.4a show two such cases, where the error increases sharply at  
677 two and one points respectively.

678 **“Nearly” PSD assumption.** In the literature, it is commonly assumed that  $A$  is  
679 “nearly” positive definite, where only a few eigenvalues are non-positive, and those  
680 are close to zero. This gives rise to the common mitigation of setting a lower-bound  
681  $\eta_0$  such that  $(A + \eta I)$  is positive definite for  $\eta > \eta_0$ . This may render an otherwise  
682 well-behaved model vacuous. The third plot in Figure 2.4a illustrates this: the model  
683 is not vacuous when unregularized, but is vacuous in the domain  $\eta > 10^{-2}$  where  
684 divergence is prohibited.

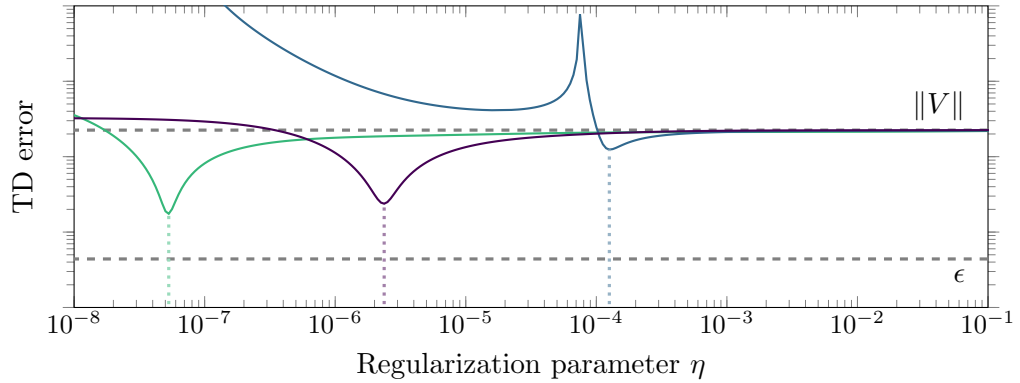
685 **The problem of a fixed  $\eta$ .** A common practice in the literature is to set  $\eta$  before  
686 training, without regard for the sampling distribution. This is ill advised, as the value  
687 may be under- or over-regularizing depending on the sampling distribution. One such  
688 example is illustrated in Figure 2.4b, where selecting an  $\eta$  that minimizes the error  
689 for one distribution will lead to vacuous or nearly-vacuous results in the other two.  
690 A second example in Figure 2.2b has no single  $\eta$  for which trajectories 2 and 3 are  
691 both non-vacuous. This is especially relevant as regularization is commonly used to  
692 permit distribution drift during training, as discussed in Section 2.4. If the training  
693 distribution changes while  $\eta$  is fixed, then algorithms that can be proven to converge  
694 to good solutions under some original distribution may converge to poor solutions as  
695 the distribution drifts.

### 696 **2.3.3 Emphatic approaches and our counterexample**

697 Emphatic-TD eliminates instability from off-policy sampling by reweighing incoming  
698 data so it appears to be on-policy. There is considerable interest in making this more  
699 practical, especially by learning the importance and value models simultaneously. A  
700 leading example of this work is COF-PAC [64], which uses  $\ell_2$ -regularized versions



(a) Different MPs at off-policy distributions selected to show small- $\eta$  error. The error may increase at multiple  $\eta$ , and may even occur *after* the optimal  $\eta$ .



(b) Three off-policy distributions with mutually incompatible  $\eta$ . There is no  $\eta$  at which all models are not vacuous or nearly vacuous.

Figure 2.4: We plot TD error against  $\eta$  to show small- $\eta$  errors (above) and mutually-incompatible  $\eta$  (below). We also plot the error at the limit of vacuity  $\|V\|$  and the representation error  $\epsilon$ .

701 of GTD2 [50] to learn both the value and emphasis models. The authors rely on  
702 regularization, particularly because the target policy changes during learning. This  
703 makes COF-PAC vulnerable to regularization-caused error. We illustrate this with  
704 Example 3 in which COF-PAC learns correctly when unregularized, but has large  
705 error when regularized.

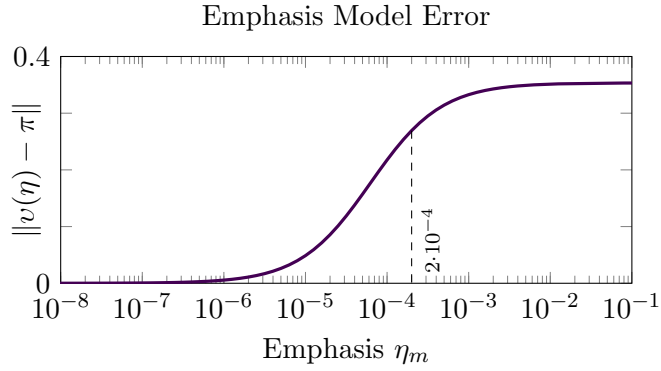
706 **Example 3.** Even if unregularized COF-PAC learns the value function with low  
707 error, regularizing it may induce arbitrarily large error.

708 *Details.* Conceptually, COF-PAC maintains two separate models that are each up-  
709 dated by TD: the emphasis and the value models. This emphasis model is used to  
710 reweigh TD updates so they appear to come from the on-policy distribution. Our  
711 strategy is to first show how regularization biases the emphasis model and then how  
712 this bias causes the value model to diverge. We begin with our three-state MP, noting  
713 its on-policy distribution is  $\pi = [.25 \ .25, \ .5]$ . We wish to learn the values using  
714 COF-PAC while sampling off-policy at  $\mu = [.2 \ .2 \ .6]$ .

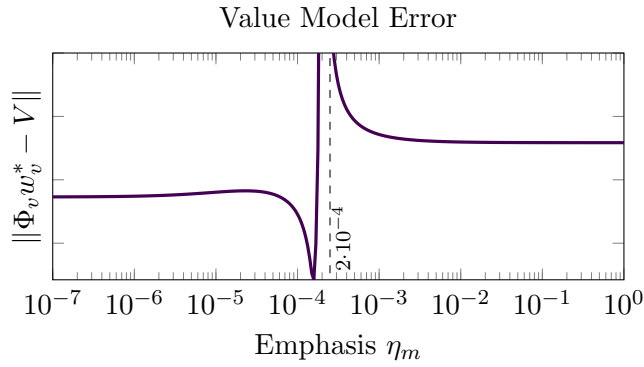
715 Now we introduce a key conceptual tool:  $v(\eta_m)$ , which is the effective distribution  
716 seen by the TD-updates, as a function of the emphasis regularization parameter  
717  $\eta_m$ . Unregularized, COF-PAC is able to resample off-policy updates to the on-policy  
718 distribution:  $v(0) \equiv \pi$ . If the model is regularized, then the effective distribution  
719 moves away from  $\pi$ . Figure 2.5a illustrates the distance between  $v(\eta_m)$  and  $\pi$  as the  
720 regularization parameter increases.

721 We can use the effective distribution to compute the error in the value model. Plotting  
722 the relationship between the value function error and  $\eta_m$  in Figure 2.5b, we can see  
723 the value function has asymptotic error around  $\eta_m = 2 \times 10^{-4}$ . This shows how  
724 COF-PAC may diverge with specific regularization.

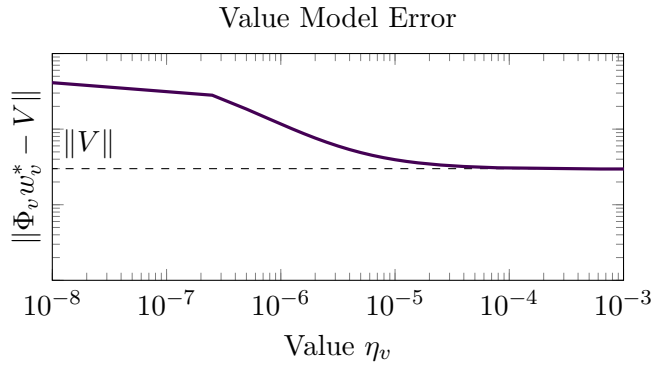
725 COF-PAC also allows for the value function to be separately regularized with param-  
726 eter  $\eta_v$ . We show the effect of this in Figure 2.5c, where the value function never does  
727 much better than  $\|V\|$  making it (nearly) vacuous. We can conclude that regularizing  
728 the emphasis model may cause the value model to diverge, and this cannot be fixed



(a)  $\eta_m$  distorts the emphasis model.

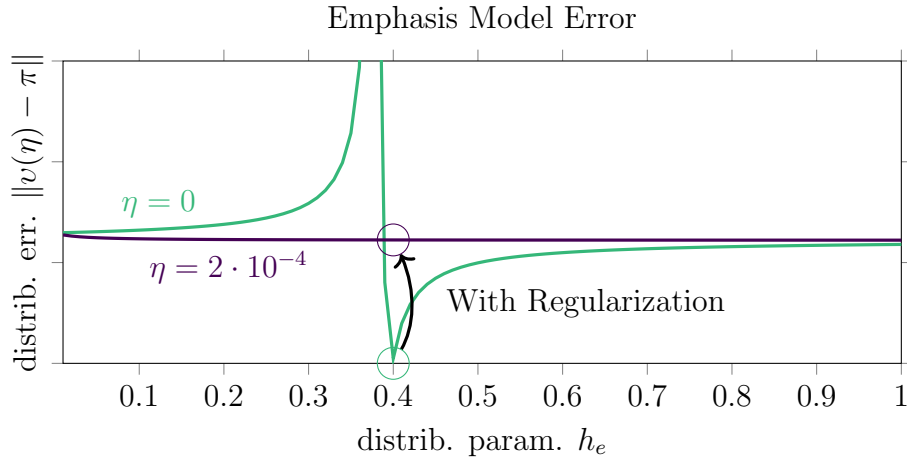


(b)  $\eta_m$  distorts value.

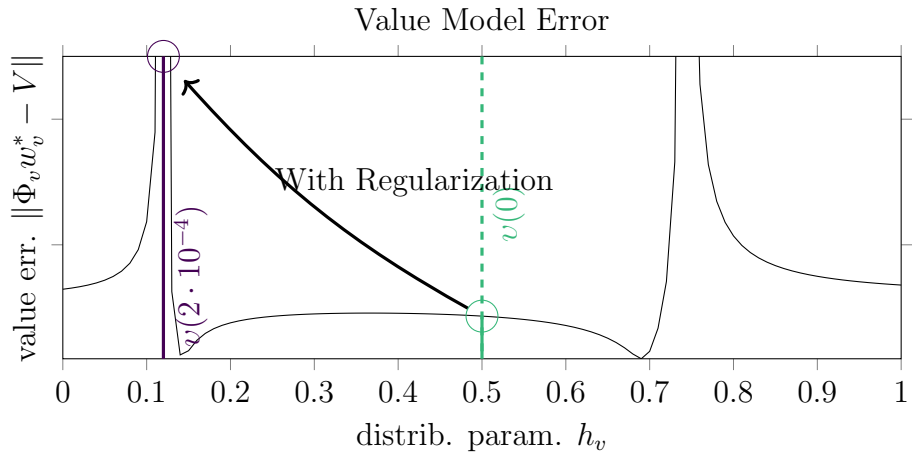


(c)  $\eta_v$  can't fix this.

Figure 2.5: Regularization on the emphasis model ( $\eta_m$ ) distorts the effective distribution (Figure 2.5a). Specific values of  $\eta_m$  induce the value function to diverge (Figure 2.5b). The resultant value function is vacuous (Figure 2.5c). Under COF-PAC, regularization can greatly increase model error.



(a) distribution is  $[h_m/2, h_m/2, (1 - h_m)]$



(b) distribution is  $[(1 - h_v)/2, h_v/2, 0.5]$

Figure 2.6: Regularization distorts the emphasis model (above), which induces the value function (below) to move to a singularity. Unregularized models are shown in green, regularized models in purple. Regularization can interact with emphasis models to significantly worsen learned value functions.

729 by regularizing the value function separately. □

730 **Mathematical details of example.** We use an MP with the same transition  
 731 function as in Figure 2.1a, with separate bases  $\Phi_m$  and  $\Phi_v$  for the emphasis and value  
 732 stages respectively. We assume that our interest in all states is uniformly  $i = 1$ .

733 We begin by setting the off-policy sampling distribution of  $\mu = [.2 \ .2 \ .6]$ , used as the  
 734 diagonal matrix  $D_\mu = \text{diag}(\mu)$ . Thanks to the simple structure of our example, we  
 735 can directly compute the emphasis as  $m = \frac{i}{1-\gamma} \cdot \pi D_\mu^{-1} \propto (5/4, 5/4, 5/6)$ . We select a  
 736 basis that allows us to represent this:

$$737 \quad \Phi_m = \begin{bmatrix} 5/4 & 0 \\ 0 & -1/100 \cdot 5/4 \\ 5/12 & -1/100 \cdot 5/12 \end{bmatrix} \quad (2.29)$$

We deliberately choose  $\Phi_m$  to have a poor condition number for reasons that will  
 738 become apparent later. We can represent  $c \cdot (5/4, 5/4, 5/6)$  exactly for any constant  $c$ :

$$739 \quad \Phi_m \cdot (1, -100) \cdot c = c \cdot (5/4, 5/4, 5/6) \quad (2.30)$$

740 Using Equation 5 from [64], we define the matrices:

$$741 \quad C_m = \Phi_m^\top D_\mu \Phi_m = \begin{bmatrix} 0.417 & -1.04 \times 10^{-3} \\ -1.04 \times 10^{-3} & 4.17 \times 10^{-5} \end{bmatrix} \quad (2.31)$$

$$742 \quad A_m = \Phi_m^\top (I - \gamma P^\top) D_\mu \Phi_m = \begin{bmatrix} 0.159 & 1.536 \times 10^{-3} \\ 1.536 \times 10^{-3} & 1.59 \times 10^{-5} \end{bmatrix} \quad (2.32)$$

And we apply these to the formulation in Lemma 3 and compute the emphasis weights  
 743 as a function of the regularization  $w_m : \mathbb{R}_0^+ \rightarrow \mathbb{R}^+$ :

$$744 \quad w_m^*(\eta) = (A_m^\top C_m^{-1} A_m + \eta I)^{-1} A_m^\top C_m^{-1} \Phi_m^\top D i \quad (2.33)$$

745 We can then use this to compute the new apparent distribution  $v(\eta)$ , which is the  
 746 effective distribution that the updates to the value model see, and it is equal to the  
 747 emphasis multiplied by the off-policy distribution.

$$748 \quad v(\eta) = \Phi_m \cdot w_m^*(\eta) \cdot D \quad (2.34)$$

749 Without any regularization, this should be exactly equal to the on-policy distribution.

$$750 \quad v(0) = [0.25 \ 0.25 \ 0.5] \equiv \pi \quad (2.35)$$

When we compute this value with a small amount of regularization  $\eta = 2 \times 10^{-4}$ , we  
 751 observe that the apparent distribution drifts far away from the on-policy distribution.

$$752 \quad v(2 \times 10^{-4}) = [0.44 \ 0.06 \ 0.5] \quad (2.36)$$

753 The proximate cause of this is the poor condition number of  $C$ , caused by the  $\frac{1}{100}$   
 754 scale factor applied to the second column of  $\Phi_m$ . This allows  $\eta$  to affect different  
 755 columns by different (relative) amounts in the definition of  $w^*(\eta)$ , which pushes it  
 756 away from the symmetric solution. This error shift is visualized in Figure 2.6a.

757 So far, we have shown how regularization causes a shift in the apparent distribution  
 758 that the TD updates see. To complete the example we show how this moves the  
 759 fixed point of the value function away from a stable point into an asymptote where it  
 760 may grow without bounds. This second phase follows in the same pattern as the first  
 761 phase, starting with the desired value function:  $V = [1 \ 2.69 \ 1.05]$  and a basis that  
 762 can nearly<sup>2</sup> represent the value function:

$$763 \quad \Phi_v = \begin{bmatrix} 1 & 0 \\ 0 & -2.69 \\ 1/2(\epsilon + 1.05) & -1/2(\epsilon + 1.05) \end{bmatrix} \quad (2.37)$$

$$764 \quad \epsilon = 2 \times 10^{-4} \quad (2.38)$$

<sup>2</sup>As before, this is necessary as it forces some amount of function approximation.

We use this basis to compute the state-rewards  $R = (I - \gamma P)V = [-0.43 \ 1.26 \ -0.38]$   
 765 and define the matrices  $A_v$  and  $C_v$  and the solution  $w_v^*(\eta)$ :

$$766 \quad A_v = \Phi_v^\top (I - \gamma P^\top) D \Phi_v \quad (2.39)$$

$$767 \quad C_v = \Phi_v^\top D \Phi_v \quad (2.40)$$

$$768 \quad w_v^*(\eta) = (A_v^\top C_v^{-1} A_v + \eta I)^{-1} A_v^\top C_v^{-1} \Phi_v^\top D R \quad (2.41)$$

We can use this solution to compute the error between the value function and the  
 true values,  $\|\Phi_v w_v(\eta) - V\|$ . First, under the correctly-resampled distribution without  
 769 regularization  $v(0) \equiv \pi$ :

$$770 \quad \Phi_v w_v^*(0)|_{D=\text{diag}(v(0))} = 0.000865 \quad (2.42)$$

771 Then, with regularization in the value function (but not in the emphasis function):

$$772 \quad \Phi_v w_v^*(2 \times 10^{-4})|_{D=\text{diag}(v(0))} = 0.0162 \quad (2.43)$$

Then, under the apparent distribution  $v(2 \times 10^{-4})$  induced by use of regularization  
 773 in the emphasis function, without and with regularization respectively:

$$774 \quad \Phi_v w_v^*(0)|_{D=\text{diag}(v(2 \times 10^{-4}))} = 418.601 \quad (2.44)$$

$$775 \quad \Phi_v w_v^*(2 \times 10^{-4})|_{D=\text{diag}(v(2 \times 10^{-4}))} = 3.00 \quad (2.45)$$

776 It is immediately obvious that the use of regularization in the emphasis function  
 777 causes the learned value function to be incorrect. Including a regularizing term in the  
 778 value estimate is not sufficient to fix the value function. This completes the example.

### 779 **The non-expansion condition and our counterexample.**

780 COF-PAC makes the strong assumption that Kolter’s non-expansion condition [24,  
 781 eqn. 10] holds in both the emphasis and value models [64, asm. 4]. This is itself a  
 782 very strong condition because it inherently assumes that both the emphasis and value

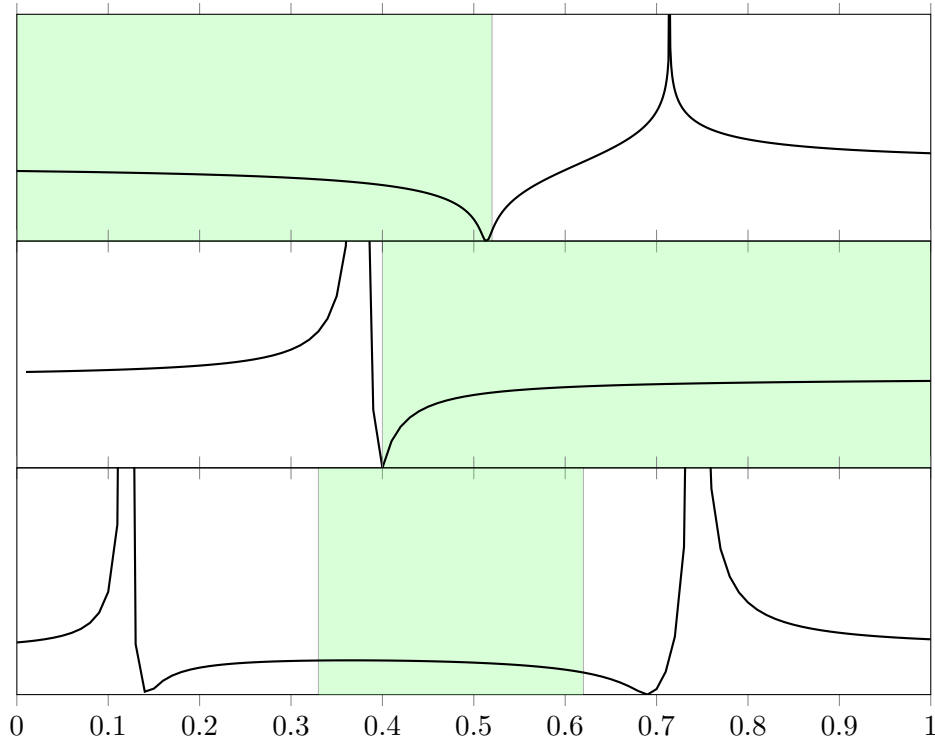


Figure 2.7: The non-expansion condition holds in the shaded region of each graph. These correspond to Figure 2.3, Figure 2.6a, and Figure 2.6b respectively.

783 models are not subject to runaway TD [64, asm. 4]. This condition selects a convex  
 784 subset of distributions under which one-step transition followed by projection onto  $\Phi$  is  
 785 non-expansive. We illustrate these regions in Figure 2.7. Even in the one-dimensional  
 786 parameterization shown, this condition only holds in a small sub-region of the space,  
 787 which suggests that it is a very strong condition.

### 788 2.3.4 Applied to multi-layer networks

789 We use a 9-state variant of our example to study the deadly triad in multi-layer neural  
 790 networks (NNs). The MDP and its transition function are depicted in Figure 2.9; we  
 791 have transformed the original MDP by replacing each self-loop with two additional  
 792 states, forming a clique with the original state. We also define a deterministic

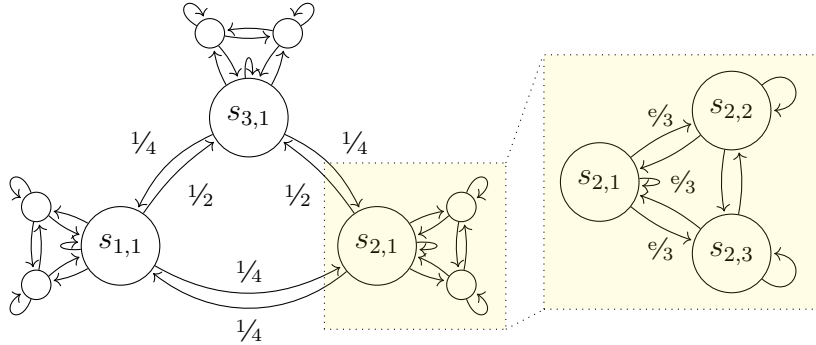


Figure 2.8: Our three-state counter-example MP is extended to nine states to illustrate how the deadly triad problem could manifest in multi-layer neural networks. The self-loop in the original example is replaced with a clique with uniform transitions except as labelled with the original edge weight  $e$ .

$$\frac{1}{12} \begin{bmatrix} 1 & 1 & 1 & 3 & & 6 \\ 4 & 4 & 4 & & & \\ 4 & 4 & 4 & & & \\ 3 & & & 1 & 1 & 1 & 6 \\ & & & 4 & 4 & 4 & \\ & & & 4 & 4 & 4 & \\ 3 & & & 3 & & & 2 & 2 & 2 \\ & & & & & & 4 & 4 & 4 \\ & & & & & & 4 & 4 & 4 \end{bmatrix}$$

(a) Transition function of the MDP.

$$\frac{1}{2} \begin{bmatrix} 1 & & & 1 \\ & 1 & & 1 \\ & & 1 & 1 \\ 1 & & & 1 \\ & 1 & & 1 \\ & & 1 & 1 \\ 1 & & & 1 \\ & 1 & & 1 \\ & & 1 & 1 \end{bmatrix}$$

(b) Observation function of the MDP.

Figure 2.9: Our three-state counterexample Markov Process. We use this to illustrate how TD models can fail despite common mitigating strategies with linear function approximation.

793 observation function  $o : \mathcal{S} \rightarrow \mathbb{B}^6$ . where each state is encoded as the concatenation of  
794 the one-hot vector of its subscripts. The value function is assigned pseudo-randomly  
795 in range  $[-1, 1]$ , and a consistent reward function is computed. We select the family  
796 of sampling distributions  $\mu \propto [4h, h, h, 4h, h, h, 8(1-h), 4(1-h), 4(1-h)]$ , where  
797 the on-policy distribution is at  $h = 0.5$ .

798 We train a simple two-layer neural network with 3 neurons in the hidden layer. The  
799 value function is assigned randomly in range  $[-1, 1]$ .

800 **Example 4.** Vacuous models and small- $\eta$  error also occur in neural network condi-  
801 tions.

802 *Details.* We train 100 models using simple semi-gradient TD updates under a fixed  
803 learning rate. We plot the mean and the 10<sup>th</sup>–90<sup>th</sup> percentile range in Figure 2.10a,  
804 with and without regularization. TD is known to exhibit high variance, and regular-  
805 ization is the traditional remedy for that. We corroborate this by noting that the  
806 performance of the unregularized model varies widely, but regularization leads to  
807 similar performance across initializations at the cost of increased error.

808 First, we show that vacuous models may exist in the neural network case. In  
809 Figure 2.10a, note how there are some off-policy distributions under which both the  
810 regularized and unregularized models perform worse than the threshold of vacuity.  
811 This is numerical verification that vacuous models exist. Second, we show the small- $\eta$   
812 error problem in the neural network case in Figure 2.10b, where we plot the TD  
813 error against  $\eta$  at a fixed off-policy distribution. We observe that around  $\eta \approx 10^{-3}$   
814 the TD Error unexpectedly *increases* before decreasing, which clearly illustrates this  
815 phenomenon.  $\square$

816 We wish to learn the model with a two-layer network with  $k < n$  nodes in the inner  
817 layer. We define the network as  $f(o(s_{i,j})) = \tan^{-1}(o(s_{i,j}) * \omega_1) * \omega_2$ . The parameters  
818  $\omega_1 \in \mathbb{R}^{6 \times k}$ ,  $\omega_2 \in \mathbb{R}^{k \times 1}$  are trained to convergence using simple TD updates with  
819 semi-gradient updates, a fixed learning rate, and without a target network.

820 In addition to the example in Figure 2.10b, we present an additional example in

821 Figure 2.11. The same Markov process, at a different off-policy distribution, attains  
822 a curve where the non-vacuous region lies before the divergent region, similar to  
823 the second row in Figure 2.4a. An added observation is that these two graphs are  
824 mutually incompatible – there is no fixed  $\eta$  that can simultaneously do better than  
825 vacuity in both, which promotes the idea of testing multiple regularization parameters  
826 or using an adaptive regularization scheme.

### 827 **2.3.5 Over-parameterization does not solve this problem**

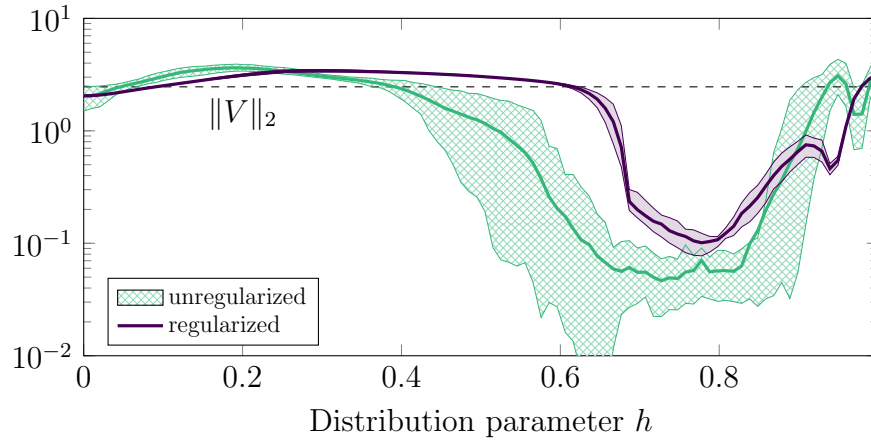
828 Baird’s counterexample [59] shows how, in the linear case, that off-policy divergence  
829 can also happen with over-parameterization, as long as some amount of function  
830 approximation occurs. It is not obvious that this conclusion persists in the neural  
831 network case, so we include an additional example showing that small- $\eta$  divergence is  
832 not solved by over-parameterization.

833 In Figure 2.12 we plot models with 3 to 13 nodes in the hidden layer. For reference,  
834 the MDP has 9 states, so some models under-parameterize and some models over-  
835 parameterize. We observe that, in the low-regularization regime, increasing the  
836 number of parameters improves the error slightly. However, increasing the number  
837 of parameters in the hidden layer does not change the behavior in the the small- $\eta$   
838 divergence region.

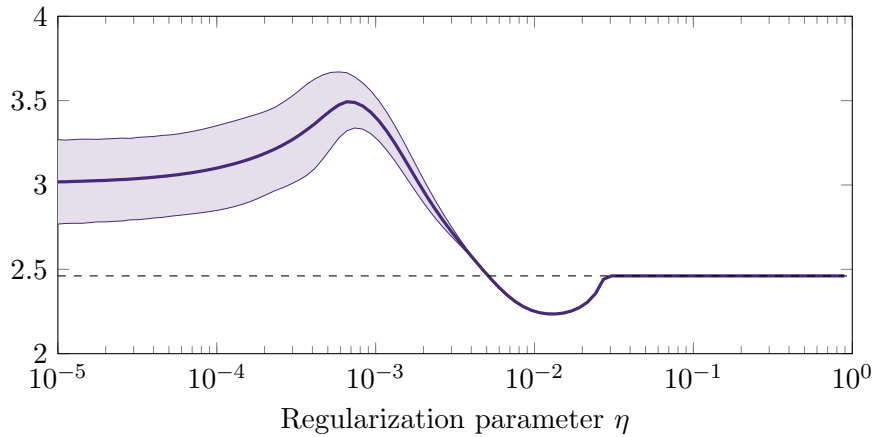
839 These qualitative links show a clear connection between the neural network case  
840 and the linear case, and highlights the importance of correctly handling off-policy  
841 sampling.

## 842 **2.4 Related Work**

843 Three examples of the deadly triad are common in the literature: the classic  
844 Tsitsiklis and Van Roy  $(w, 2w)$  example [48, p. 260], Kolter’s example [24], and  
845 Baird’s counterexample which shows how training instability can exist despite over-  
846 parameterization [59].



(a) Mean and 10<sup>th</sup>–90<sup>th</sup> percentile errors of 100 NN value models trained to convergence.



(b) The relationship between error and  $\eta$  at the off-policy distribution  $h = 0.31$ .

Figure 2.10: We illustrate how regularization interacts with NN value functions, showing that the problems identified in this chapter persist in the NN case.

847  $\ell_2$  regularization is common when proving that an algorithm converges under a  
848 changing sampling policy. This is seen in GTD (analyzed in [61]), GTD2 [50], RO-  
849 TD [33], and COF-PAC [64]. This assumption may also be used to ensure convergence  
850 when training with a target network [63]. Despite the prevalence of regularization,  
851 the induced bias from using it is not well studied. It is often dismissed as a mere  
852 technical assumption, as in [8]. In this chapter, we contradict that and show how  
853 regularization may induce catastrophic bias. By showing concrete examples, this  
854 work hopes to inspire further investigation into regularization-induced bias in the  
855 same vein as [61].

856 **Alternatives to regularization and TD** We focus on  $\ell_2$  regularization in this  
857 chapter, which penalizes the  $\ell_2$ -norm of the learned weights; it is also possible to  
858 use  $\ell_1$  regularization with a proximal operator/saddle point formulation as in [33],  
859 or any convex regularization term under a fixed target policy [61]. Instead of  
860 directly regularizing the weights, COP-TD uses a discounted update [13]. DisCor [25]  
861 propagates bounds on Q-value estimates to quickly converge TD learning in the  
862 face of large bootstrapping error; it is not clear if DisCor can overcome off-policy  
863 sampling. A separate primal-dual saddle point method has also been adapted to  $\ell_2$   
864 regularization [9] and is known to converge under deadly triad conditions, and recent  
865 work [57] has derived error bounds with improved scaling properties in the linear  
866 setting, offering a promising line of research.

867 Emphatic-TD [49] fixes the fundamental problem in off-policy TD by reweighing  
868 updates so they appear on-policy. The core idea underlying these techniques is to  
869 estimate the “follow-on trace” for each state, the (weighted,  $\lambda$ - and  $\gamma$ -discounted)  
870 probability mass of all states whose value estimates it influences. This trace is then  
871 used to estimate the emphasis, which is the reweighing factor for each update. While  
872 this family of methods is provably optimal in expectation, it is subject to tremendous  
873 variance in theory and practice, especially when the importance is estimated using  
874 Monte-Carlo sampling.<sup>3</sup> In practice, these methods learn the follow-on trace using

<sup>3</sup>Sutton and Barto’s textbook [48] says about Emphatic-TD applied to Baird’s example that “it is nigh impossible to get consistent results in computational experiments.”

875 TD [19, 64] or similar [17], which makes them vulnerable to bias induced by the use  
876 of regularization.

## 877 **2.5 Relationship to modern RL algorithms**

878 It is still not obvious how strongly this instability affects modern RL algorithms,  
879 which are also sensitive to a variety of other failure modes. Unlike our examples,  
880 the sampling distribution changes during training, and regularization mechanisms  
881 are more complex than simple  $\ell_2$  penalties. The exact relationship between the  
882 instabilities we study and RL algorithms is an open problem, but we offer two pieces  
883 of indirect evidence suggesting there is a link.

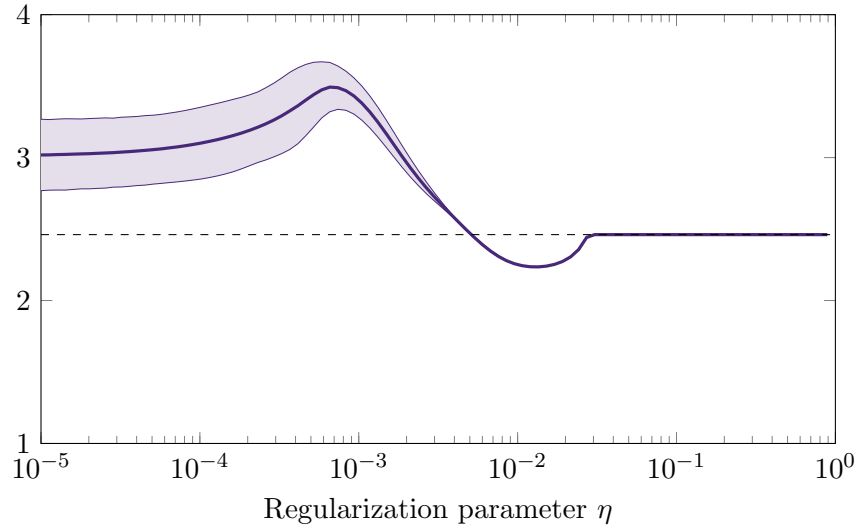
884 First, in the offline/batch RL literature, it is well-known that online RL algorithms  
885 naively applied can catastrophically fail if the learned policy is not consistent with  
886 the data distribution. This is known as the distribution shift problem, [31, p. 26] and  
887 offline RL algorithms are generally constructed to explicitly address this. Second,  
888 when using experience replay buffers in online RL algorithms, policy quality generally  
889 improves when older transitions are more quickly evicted [10]. However, there are  
890 multiple factors at work here, and it is not possible to cleanly separate the instability  
891 from off-policy sampling from the remaining factors.

## 892 **2.6 Conclusion**

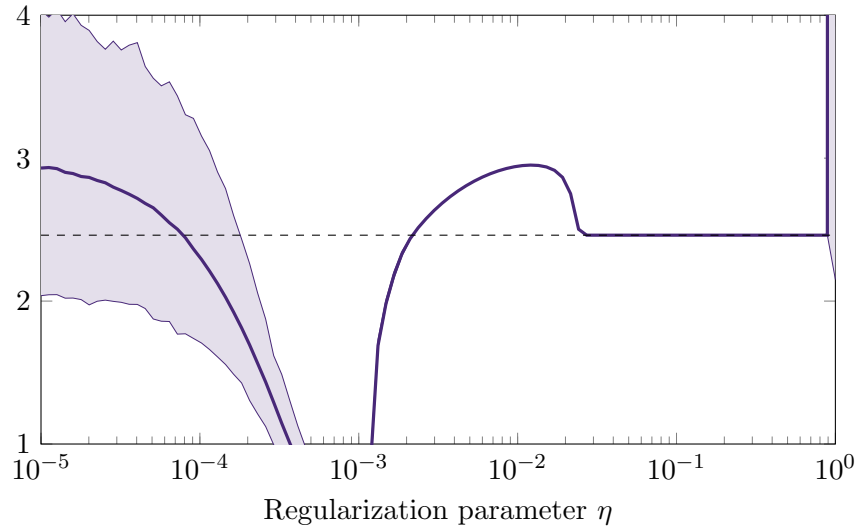
893 There is a tremendous focus in the RL literature on proving convergence of novel  
894 algorithms, but not on the error at convergence. Papers like [63] are laudable  
895 because they provide error bounds; even if the current bounds are loose, future  
896 work will no doubt tighten them. In this work, we show that the popular technique  
897 of  $\ell_2$  regularization does not always prevent singularities and could even introduce  
898 catastrophic divergence. We show this with a new counterexample that elegantly  
899 illustrates the problems with learning off-policy and how it persists into the NN case.  
900 Even though regularization can catastrophically fail in the ways we illustrate, it

901 remains a reasonable method that may offer a fair tradeoff—as long as we are careful  
902 to check that we are not running afoul of the failure modes we explain here. It may be  
903 possible to design an adaptive regularization scheme that can avoid these pathologies.  
904 For now, testing the model performance over a range of regularization parameters  
905 (spanning several orders of magnitude) is the best option we have to detect such  
906 pathological behavior.

907 Emphatic-TD is perhaps the most promising area of research for mitigating off-policy  
908 TD-learning. The key problem preventing its widespread adoption is the difficulty  
909 in estimating the emphasis function, but future work in this area may be able to  
910 overcome this. Our example shows the risk of relying on regularization in practical  
911 implementations of such methods. It is absolutely critical that Emphatic algorithms  
912 correctly manage regularization to avoid the risks that we highlight here.

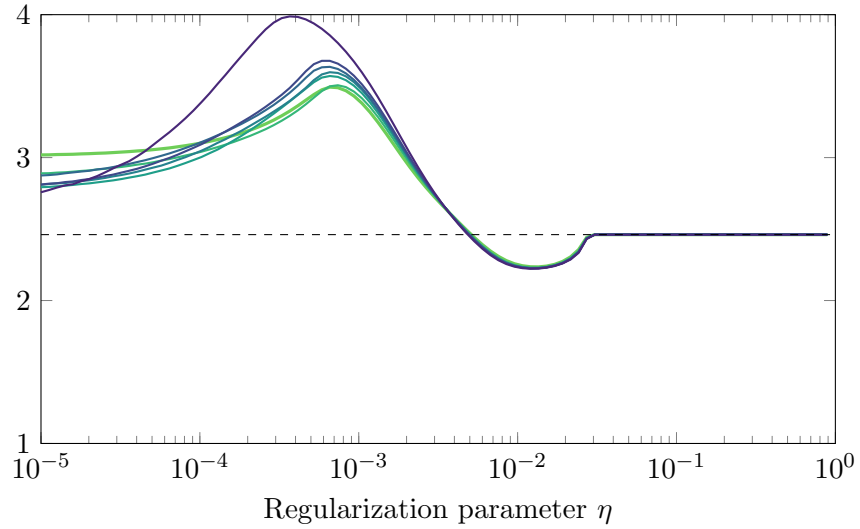


(a)  $h = 0.31$  (From Figure 2.10b)

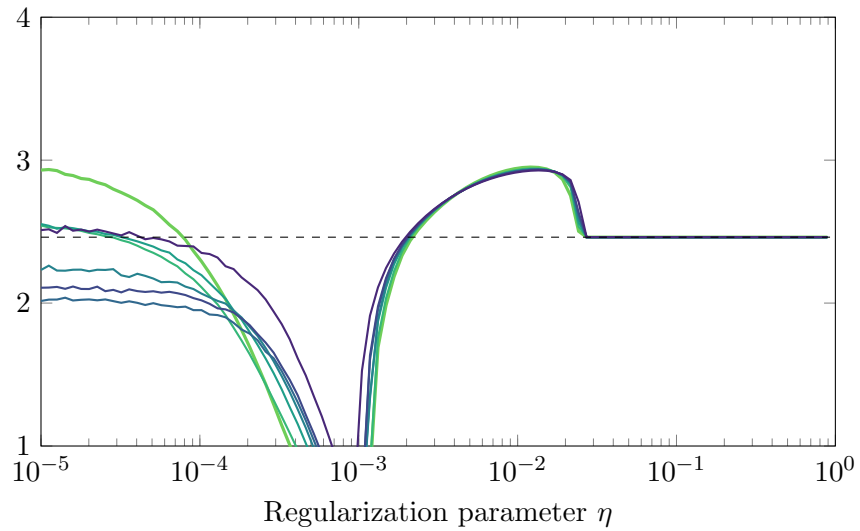


(b)  $h = 0.95$

Figure 2.11: The relationship between error and  $\eta$  at different off-policy distributions, showing mutually incompatible regularization behavior. The shaded range indicates the region between the 5th and 95th percentile of 100 differently-initialized models.



(a)  $h = 0.31$



(b)  $h = 0.95$

Figure 2.12: The relationship between  $\eta$  and error with different amount of model parameterization (with 3, 5, 7, 9, 11, 13, and 64 nodes in the hidden layer, corresponding to darkening colors.)

## 913 Chapter 3

# 914 Projected Off-Policy TD for Offline 915 Reinforcement Learning

916 A key problem in offline Reinforcement Learning (RL) is the mismatch between the  
917 dataset and the distribution over states and actions visited by the learned policy,  
918 called the *distribution shift*. This is typically addressed by constraining the learned  
919 policy to be close to the data generating policy, at the cost of performance of the  
920 learned policy. We propose Projected Off-Policy TD (POP-TD), a new critic update  
921 rule that resamples TD updates to allow the learned policy to be distant from the data  
922 policy without catastrophic divergence. Unlike Emphatic-TD and the importance  
923 sampling literature, we resample to any “safe” distribution, not necessarily the on-  
924 policy. We show how this algorithm works on a well-understood toy example from  
925 the literature, and then characterize its performance with varying parameterization  
926 on a specially-constructed offline RL task. This is a novel approach to stabilizing  
927 off-policy RL, and sets the stage for future work on larger tasks.

928 *Paper in preparation, by Manek, Roderick, and Kolter (2023)*

## 929 3.1 Introduction

930 Reinforcement Learning (RL) aims to learn policies that maximize rewards in Markov  
931 Decision Processes (MDPs) through interaction, generally using Temporal Difference  
932 (TD) methods. In contrast, offline RL focuses on learning optimal policies from a  
933 static dataset sampled following an unknown policy, possibly a policy designed for a  
934 different task. Thus, algorithms are expected to learn without the ability to interact  
935 with the environment. This is useful in environments that are expensive to explore  
936 (such as running a Tokamak nuclear reactor [7]), or high-dimensional environments  
937 with cheap access to expert or near-expert trajectories (such as video games). Levine  
938 et al. [30] present a comprehensive survey of the area.

939 Since in offline RL the data is gathered before training begins, there is a mismatch  
940 between the the state-distributions implied by the learned policy and the data. When  
941 applying naive RL algorithms in this setting, they tend to bootstrap from regions  
942 with little or no data, causing runaway self-reinforcement. Offline RL algorithms like  
943 Conservative Q-Learning (CQL) [26] generally constrain the learned policy to remain  
944 within the support of the data. While this works well in practice, there still remains  
945 a large gap in performance between online and offline RL. One reason for this is an  
946 additional subtlety to distribution shift: because of the combination of off-policy RL  
947 and function approximation, it is possible for RL to diverge if the generating policy  
948 and the learned policy are sufficiently different even if the data has full support for  
949 the learned policy.

950 We illustrate a simple case in Figure 3.1, where a simple grid environment is designed  
951 to elicit the shortest trajectory from start (S) to goal (G). Agents can move one step  
952 in each cardinal direction, reaching the goal yields a unit reward, and the episode  
953 ends on reaching the goal or any marked cell (X). We generate a dataset by following  
954 a suboptimal data policy (---) with sufficient dithering to guarantee that every state-  
955 action pair is represented. If we use a tabular Q-function, we can recover the optimal  
956 policy (—) and obtain the true value function. When we use a linear Q-function,  
957 however, the error is much larger. We find that about half of random initializations

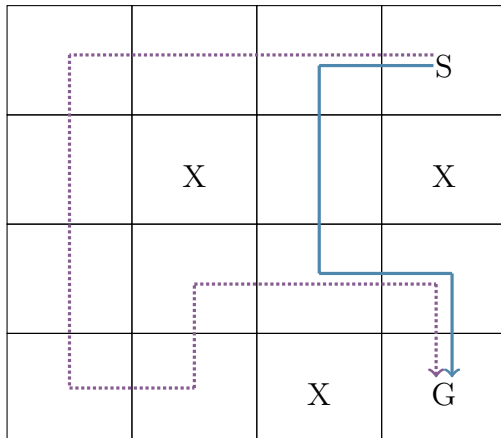


Figure 3.1: A simple grid environment illustrating distribution shift despite complete support. We wish to learn the optimal trajectory (—) from a suboptimal data policy (---) which is  $\epsilon$ -dithered to get sufficient coverage. When we apply Q-learning methods to this, training often diverges to arbitrarily poor values. This is a consequence of distribution shift. In this paper, we propose a technique to solve this divergence.

958 lead to Q-functions that either diverge or converge to large error. This shows how  
 959 even with full coverage of states and actions, distribution shift can be a significant  
 960 source of error. We provide more details in Section 3.5.1.

961 In this chapter, we introduce POP-TD, a novel method of mitigating the error from  
 962 off-policy learning. We show theoretically that this method bounds the off-policy  
 963 approximation error for TD-based RL methods. We illustrate the resampling process  
 964 on a well-known toy example, and then demonstrate its effectiveness on an example  
 965 of offline RL under distribution shift.

## 966 3.2 Related Work

967 **Off-Policy TD Learning** Instability from learning off-policy has also been studied  
 968 in the classic RL literature. First described by Tsitsiklis and Van Roy [54], the use  
 969 of TD learning, function approximation, and off-policy sampling may cause severe  
 970 instability or divergence. This is known as the *deadly triad* [48, p. 264] and even if

971 many variants of TD still converge, the quality of the solution at convergence may be  
972 arbitrarily poor [24].

973 There are three existing lines of work in the literature that attempt to resolve this:  
974 regularization, Emphatic reweighing, and TD Distribution Optimization (TD-DO).  
975 The first attempts to regularize TD, typically with  $\mathcal{L}_2$ -norm weight regularization.  
976 Alternative regularization schemes are  $\mathcal{L}_1$  [33], convex [61], and bounds propagation  
977 [25]. There are well-documented failure modes related to regularization [35]. The  
978 second line started with Emphatic-TD, in which Sutton, Mahmood, and White [49]  
979 note that it is possible to reweigh samples obtained off-policy so they appear to be  
980 on-policy. Such methods learn the follow-on trace using Monte-Carlo methods (in the  
981 original), TD [19, 64] or techniques similar to TD [17]. The third method, TD-DO,  
982 works by solving a small optimization problem on each TD update to reweigh samples  
983 to satisfy the Non-Expansion Criterion, which we introduce in the next section.

984 **Off-Policy and Offline Deep RL** Nearly all modern TD-based deep RL methods  
985 perform off-policy learning in practice. To improve data efficiency and learning  
986 stability, an experience replay buffer is often used. This buffer stores samples from  
987 previous versions of the policy [38], and so the distribution of the data is not on-policy  
988 for the current version of the policy. Additionally, exploration policies, such as a  
989 epsilon greedy [48, p. 100] or Soft Actor Critic (SAC)-style entropy regularization [15]  
990 <sup>1</sup>, are often used, which also results in off-policy learning. In practice, the difference  
991 between the current policy and the samples in the buffer is limited by setting a limit to  
992 the buffer size and discarding old data; or by keeping the exploration policy relatively  
993 close to the learned policy. In practice, this is sufficient to prevent outright divergence,  
994 though the extent to which it decreases performance is not well-understood.

995 However, in the offline RL setting where training data is static, there is usually a  
996 much larger discrepancy between the state-action distribution of the data and the  
997 distribution induced by the learned policy. This discrepancy presents a significant

<sup>1</sup>While the original SAC algorithm is technically on-policy since it learns an entropy-regularized value function, the entropy-regularization is often dropped from the value-function estimate in practice to improve performance.

998 challenge for offline RL [30]. While this distributional discrepancy is often presented  
999 as a single challenge for offline RL algorithms, it is convenient to separate the two  
1000 distinct aspects of this challenge and address them independently: *support mismatch*  
1001 and *proportional mismatch*. When the support of the two distributions differ, learned  
1002 value functions will have arbitrarily high errors in low-data regions. Support mismatch  
1003 is dealt with by either constraining the KL-divergence between the data and learned  
1004 policies [11, 28, 60], by penalizing or pruning low-support (or high-uncertainty) actions  
1005 [26, 62, 22].

1006 Even when the support of the data distribution matches that of the policy distribution,  
1007 naive TD methods can produce unbounded errors in the value function [54]. We call  
1008 this challenge *proportional mismatch*.

1009 Importance sampling (IS) [44] is one of the most widely used techniques to address  
1010 proportional mismatch. The idea with IS is to compute the differences between the  
1011 data and policy distributions for every state-action pair and re-weight the TD updates  
1012 accordingly. However, these methods suffer from variance that grows exponentially in  
1013 the trajectory length. Several methods have been proposed to mitigate this challenge  
1014 and improve performance of IS in practice [16, 13, 40, 39, 32], but the learning is still  
1015 far less stable than other offline deep RL methods. In this work, we propose a new  
1016 method to bound the value-function approximation errors caused by proportional  
1017 mismatch without the need to explicitly compute (or approximate) IS weights.

### 1018 3.3 Problem Setting and Notation

1019 Consider the  $n$ -state Markov chain  $(\mathcal{S}, P, R, \gamma)$ , with finite state space  $\mathcal{S}$ , transition  
1020 function  $P : \mathcal{S} \times \mathcal{S} \rightarrow \mathbb{R}_+$ , reward function  $R : \mathcal{S} \rightarrow \mathbb{R}$ , and discount factor  $\gamma \in [0, 1]$ .  
1021 Because the state-space is finite, it can be indexed as  $\mathcal{S} = \{1, \dots, n\}$ . This allows  
1022 us to use matrix rather than operator notation. The expected  $\gamma$ -discounted future  
1023 reward of being in each state  $V(s) := \mathbb{E}[\sum_{t=0}^{\infty} \gamma^t R(s_t) | s_0 = s]$  is called the value

1024 function. The value function is consistent with Bellman’s equation (in matrix form):

$$1025 \quad V = R + \gamma PV \quad (3.1)$$

1026 In the linear setting, we approximate the value function as  $V(s) \approx w^\top \phi(s)$ , where  
1027  $\phi : \mathcal{S} \rightarrow \mathbb{R}^k$  is a fixed basis function and we estimate parameters  $w \in \mathbb{R}^k$ . In matrix  
1028 notation, we write this as  $V \approx \Phi w$ .

1029 In this work, we are interested in the offline learning setting, where the sampling  
1030 distribution  $\mu$  differs from the stationary distribution  $\nu$ . In this setting, the previous  
1031 equation is insufficient. We need to account for the function approximation, and so  
1032 the TD solution is:

$$1033 \quad \Phi w = \Pi_\mu(R + \gamma P\Phi w) \quad (3.2)$$

1034 where  $\Pi_\mu = \Phi(\Phi^\top D_\mu \Phi)^{-1} \Phi^\top D_\mu$  is the projection onto the column space of  $\Phi$  weighted  
1035 by the data distribution  $\mu$  through the matrix  $D_\mu = \text{diag}(\mu)$ . This projection may be  
1036 arbitrarily far from the true solution, and so the error may be correspondingly large.  
1037 The literature bounds the error as:

1038 **Theorem 2.** *The error at the TD fixed point is  $\|\Phi w - V\|_{D_\mu}$ . Lemma 6 from [54]*  
1039 *bounds this in terms of error projecting  $V$  onto the column space of  $\Phi$ :*

$$1040 \quad \|\Phi w - V\|_{D_\mu} \leq \frac{1}{1 - \gamma} \|\Pi_\mu V - V\|_{D_\mu} \quad (3.3)$$

1041

### 1042 3.3.1 The Non-Expansion Criterion (NEC)

1043 Thus far we have left open the notion of a “safe” distribution to resample TD updates  
1044 to. The on-policy distribution is always safe, but we need to establish some criterion  
1045 for “safe” off-policy distributions. Tsitsiklis and Van Roy lay the groundwork for  
1046 this by analyzing the training of on-policy TD as a dynamical system and showing

1047 that once TD reaches its fixed point, subsequent TD updates form a non-expansive  
 1048 mapping around that fixed point (1996, lemma 4), and therefore prove that on-policy  
 1049 TD does not diverge.

1050 To do this, they begin with the fact that error bounds from on-policy TD follow  
 1051 the property that the  $D$ -norm of any vector  $x \in \mathbb{R}^n$  is non-expansive through the  
 1052 transition matrix. That is:  $\|Px\|_D \leq \|x\|_D$ , where  $D = \text{diag}(\pi)$ . Kolter [24] extend  
 1053 this analysis to the off-policy case, deriving a linear matrix inequality (LMI) under  
 1054 which the TD updates are guaranteed to be non-expansive around the fixed point.  
 1055 This is the Non-Expansion Criterion (2011):

$$1056 \quad \|\Phi w - V\|_D \leq \frac{1 + \gamma \kappa(D^{-1/2} D^{1/2})}{1 - \gamma} \|\Pi_D V - V\|_D \quad (3.4)$$

1057 From this bound, he derives the *non-expansion criterion* (NEC):

$$1058 \quad \|\Pi_D P \Phi w\|_D \leq \|\Phi w\|_D \quad (\forall w \in \mathbb{R}^n) \quad (3.5)$$

1059 This holds if and only if the matrix  $F_D$  is positive semi-definite

$$1060 \quad F_D \equiv \begin{bmatrix} \Phi^\top D \Phi & \Phi^\top D P \Phi \\ \Phi^\top P^\top D \Phi & \Phi^\top D \Phi \end{bmatrix} \succcurlyeq 0 \quad (3.6)$$

1061 Equivalently, in terms of the expectation over states:

$$1062 \quad \mathbb{E}_{s \sim \mu, s' \sim p(\cdot|s)} \left[ \begin{bmatrix} \phi(s)\phi(s)^\top & \phi(s)\phi(s')^\top \\ \phi(s')\phi(s)^\top & \phi(s)\phi(s)^\top \end{bmatrix} \right] \succcurlyeq 0. \quad (3.7)$$

1063 This constraint describes a convex subset of  $D$ . As a  $2k \times 2k$  matrix (where  $k$  is the  
 1064 number of features),  $F$  is prohibitively large to enumerate for any real RL problem,  
 1065 and so our algorithm is designed to make use of this without ever constructing it  
 1066 directly. Further, we notice that the construction of  $F_D$  depends on  $P$ , the transition  
 1067 matrix of the underlying Markov process, which makes our algorithm more complex.

1068 For convenience, we write this as:

$$1069 \quad \mathbb{E}_{s \sim q}[F(s)] \succcurlyeq 0, \text{ where} \tag{3.8}$$

$$1070 \quad F(s) = \mathbb{E}_{s' \sim p(s'|s)} \left[ \begin{bmatrix} \phi(s)\phi(s)^\top & \phi(s)\phi(s')^\top \\ \phi(s')\phi(s)^\top & \phi(s)\phi(s)^\top \end{bmatrix} \right]$$

1071 NEC is an expectation over some state distribution  $q$  and transition distribution  
 1072  $p(s, s') = p(s'|s)\mu(s)$ . Because it is an LMI, the satisfying state distributions  $q$  form  
 1073 a convex subset.

1074 Directly constructing  $F(s)$  or  $F(s, s')$  is impossible on all but the simplest examples –  
 1075 it would take  $\mathcal{O}(k^2n)$  or  $\mathcal{O}(k^2n^2)$  memory respectively to hold all the necessary data.  
 1076 Instead we exploit the structure inherent in the problem to make use of  $F(s)$  without  
 1077 creating it.

### 1078 **3.4 Projected Off-Policy TD (POP-TD)**

1079 We propose an alternative approach to stabilizing off-policy training, based on the  
 1080 NEC by Kolter [24]. POP-TD identifies a convex set of “safe” distributions that  
 1081 satisfy NEC and reweighs TD updates to come from that set. In contrast to TD-DO,  
 1082 POP-TD solves a different optimization problem using a two-timescales update with  
 1083 fixed cost per iteration, allowing it to scale to real-world problems.

1084 We begin by deriving the projected off-policy update for Markov Chains without  
 1085 a separate policy function. We will extend this derivation to support actions and  
 1086 Markov Decision Processes (MDPs) in Section 3.4.5. Our algorithm resamples TD  
 1087 updates so they come from some distribution  $q$  for which the NEC holds. Given input  
 1088 data  $(x_1, x_2, \dots)$ , this is the same as finding a set of weights  $q_1, q_2, \dots$  such that

$$1089 \quad \sum_i q_i \cdot F(x_i) \succcurlyeq 0 \tag{3.9}$$

### 1090 3.4.1 I- and M-projections

1091 The Kullback-Leibler divergence is an *asymmetric* measure, and so it is usually  
1092 the case that  $\min_q \text{KL}(q||\mu) \neq \min_q \text{KL}(\mu||q)$ . The former (“from  $\mu$  to  $q$ ”) is  
1093 an information (or I-)projection, which tends to under-estimate the support of  $q$   
1094 potentially excluding possible sampling distributions to reweigh to. The latter (“from  
1095  $q$  to  $\mu$ ”) is a moment (or M-)projection, which tends to over-estimate the support of  
1096  $q$  and avoid zero solutions. In our solution, we are proposing using an I-projection  
1097 instead of the M-projection used by Kolter [24].

### 1098 3.4.2 Optimizing the distribution

1099 In the previous section we have characterized a convex subset of off-policy distributions  
1100 under which TD learning is guaranteed not to diverge. If we can discover any such  
1101 distribution for a particular TD problem, we can reweigh our TD updates (from any  
1102 distribution) so they appear consistent with this reweighing distribution. This is  
1103 related to the main insight in Emphatic-TD [49], with the key innovation that we  
1104 can take any non-expansive distribution *not just the on-policy distribution*.

1105 We can now write down the optimization problem that we wish to solve:

$$1106 \quad \underset{q}{\text{minimize}} \text{KL}(q||\mu) \quad \text{s.t.} \quad \mathbb{E}_{s \sim q}[F(s)] \succeq 0 \quad (3.10)$$

1107 We are searching for  $q$ , the closest distribution to the sampling distribution  $\mu$  such  
1108 that  $F$  is PSD under  $q$ . Note that we could in principle minimize any notion of  
1109 “closest” to find some satisfying distribution – for example Kolter [24] explores the  
1110 effects of minimizing  $\text{KL}(\mu||q)$ .

1111 We construct the dual of this problem:

$$1112 \quad \underset{Z \succ 0}{\text{maximize}} \underset{q}{\text{minimize}} \text{KL}(q||\mu) - \text{tr} Z^\top \mathbb{E}_{s \sim q}[F(s)] \quad (3.11)$$

1113 Using the Lagrange multiplier  $Z \in \mathbb{R}^{2k \times 2k}$ , we solve the inner optimization problem:

$$1114 \quad \underset{q}{\text{minimize}} \quad -H(q) - \mathbb{E}_{s \sim q}[\log \mu(s) + \text{tr} Z^\top F(s)] \quad (3.12)$$

1115 Writing down Lagrangian and solving for the optima, we obtain:

$$1116 \quad q^*(s) \propto \mu(s) \exp(\text{tr} Z^\top F(s)) \quad (3.13)$$

1117 (Subject to the normalization constraint that  $\sum_{s \in \mathcal{S}} q^*(s) = 1$ .)

1118 Plugging this back into our dual formulation, we obtain the optimization problem:

$$1119 \quad \underset{Z \succcurlyeq 0}{\text{maximize}} \quad -\log \mathbb{E}_{s \sim \mu}[\exp(\text{tr} Z^\top F(s))] \quad (3.14)$$

1120 Which we can simplify to

$$1121 \quad \underset{Z \succcurlyeq 0}{\text{minimize}} \quad \mathbb{E}_{s \sim \mu}[\exp(\text{tr} Z^\top F(s))] \quad (3.15)$$

1122 As discussed earlier,  $F(s)$  cannot be directly constructed; instead, we assume that  $Z$   
 1123 holds a specific structure and optimize the problem.

### 1124 **3.4.3 The structure of $Z$**

1125 Our next goal is to transform this constrained optimization problem into an uncon-  
 1126 strained problem over a low-rank version of  $Z$ , suitable for learning via SGD.

1127 We assume (and later check!) that the solution for  $Z$  is low-rank. Intuitively, this is  
 1128 because  $\mathbb{E}_{s \sim \mu}[F(s)]$  is PSD when  $\mu$  is close to  $\pi$ , and for most MDPs, sampling off-  
 1129 policy leads to only a small number of negative eigenvalues that need to be corrected  
 1130 by  $Z$ . Kolter [24] provides a technical explanation: by the KKT conditions,  $Z$  will  
 1131 have rank complementary to  $\mathbb{E}_{s \sim \mu}[F(s)]$ , and the latter is expected to be full rank. It  
 1132 is worth noting that this “almost-PSD” assumption is common in the field.

1133 We make the mild assumption that  $Z$  has rank  $m$ , where  $m \ll k$ . We apply the  
 1134 Burer-Montiero approach [4] to convert the constrained optimization problem over  $Z$   
 1135 into an unconstrained optimization over low-rank matrices  $A \in \mathbb{R}^{k \times m}$  and  $B \in \mathbb{R}^{k \times m}$ :

$$1136 \quad Z^* = \begin{bmatrix} A \\ B \end{bmatrix} \begin{bmatrix} A \\ B \end{bmatrix}^T \quad (3.16)$$

1137 This allows us to represent the rank- $m$  PSD matrix  $Z^*$  in terms of the unconstrained  
 1138 matrices  $A$  and  $B$ . Substituting this into the dual formulation, we get:

$$1139 \quad \underset{A, B}{\text{minimize}} \mathbf{E}_{s \sim \mu} \left[ \exp \left( \text{tr} \begin{bmatrix} A \\ B \end{bmatrix} \begin{bmatrix} A \\ B \end{bmatrix}^T F(s) \right) \right] \quad (3.17)$$

1140 We can leverage the structure of  $F(s)$  to simplify the trace term:

$$1141 \quad \text{tr} Z^T F(s) \quad (3.18)$$

$$1142 \quad = \text{tr} \begin{bmatrix} A \\ B \end{bmatrix}^T \begin{bmatrix} A \\ B \end{bmatrix}^T F(s) \quad (3.19)$$

$$1143 \quad = \text{tr} \begin{bmatrix} A \\ B \end{bmatrix}^T F(s) \begin{bmatrix} A \\ B \end{bmatrix} \quad (3.20)$$

$$1144 \quad = \text{tr} \begin{bmatrix} A \\ B \end{bmatrix}^T \mathbf{E}_{s' \sim p(s'|s)} \begin{bmatrix} \phi(s)\phi(s)^T & \phi(s)\phi(s')^T \\ \phi(s')\phi(s)^T & \phi(s)\phi(s)^T \end{bmatrix} \begin{bmatrix} A \\ B \end{bmatrix} \quad (3.21)$$

$$1145 \quad = \text{tr} [(A + B)^T \phi(s)\phi(s)^T (A + B) - 2B^T \mathbf{E}_{s' \sim p(s'|s)} [\phi(s)(\phi(s) - \phi(s'))^T] A] \quad (3.22)$$

$$1146 \quad = \|(A + B)^T \phi(s)\|^2 - \text{tr} [2B^T \mathbf{E}_{s' \sim p(s'|s)} [\phi(s)(\phi(s) - \phi(s'))^T] A] \quad (3.23)$$

1147 This allows us to rewrite the optimization problem as:

$$1148 \quad \underset{A, B}{\text{minimize}} \mathbf{E}_{s \sim \mu} \left[ \exp \left( \begin{array}{c} \|(A + B)^T \phi(s)\|^2 \\ -\text{tr} [2B^T \mathbf{E}_{s' \sim p(s'|s)} [\phi(s)(\phi(s) - \phi(s'))^T] A] \end{array} \right) \right] \quad (3.24)$$

1149 where the small parameters  $A$  and  $B$  can be optimized with regular gradient-descent  
1150 methods.

### 1151 3.4.4 Update rules

1152 We can't directly optimize our problem because that would require us to estimate the  
1153 inner expectation term. Instead, we use a two-timescales approach by estimating two  
1154 mutually-dependent quantities separately and improving them at potentially different  
1155 rates. This generally converges to a valid solution with a little tuning.

1156 We choose to estimate the matrices  $A, B \in \mathbb{R}^{k \times m}$  and separately the function  $g_\theta : \mathcal{S} \in \mathbb{R}$  where

$$1158 \quad g_\theta(s) \approx \text{tr} Z^T F(s) \quad (3.25)$$

1159 which can be approximated as a linear function (or a neural network) with parameters  
1160  $\theta$ . The size of the weights learned by POP-TD are therefore  $\mathcal{O}(k)$ , comparable to the  
1161 size of vanilla Q-learning.

1162 This corresponds to the auxiliary loss term for  $A, B$ :

$$1163 \quad \mathcal{L}_{A,B}(s, s') = \exp(g_\theta(s)) [\|(A + B)^T \phi(s)\|^2 - \text{tr} [2B^T \phi(s)(\phi(s) - \phi(s'))^T A]] \quad (3.26)$$

1164 and for  $g$ :

$$1165 \quad \mathcal{L}_g(s, s') = (g_\theta(s) - [\|(A + B)^T \phi(s)\|^2 - \text{tr} [2B^T \phi(s)(\phi(s) - \phi(s'))^T A]])^2 \quad (3.27)$$

1166 And finally, when updating the value function weights  $w$ , we multiply the loss  
1167 associated with each transition by  $\exp(g(s))$  to resample it so it appears to come  
1168 from the “safe” distribution, which completes the description of the algorithm!

1169 **Computing the loss** A naive implementation of the loss function will require  
1170 intermediate matrices of size  $[k \times k]$ . We can improve speed by computing the loss in

1171 terms of  $[m \times 1]$  intermediates instead. For a transition sample  $(s, s')$ , this can be  
 1172 done as:

$$\begin{aligned}
 1173 \quad M_A &= A^T \phi(s) \in \mathbb{R}^m \\
 1174 \quad M'_A &= A^T \phi(s') \in \mathbb{R}^m \\
 1175 \quad M_B &= B^T \phi(s) \in \mathbb{R}^m \\
 1176 \quad \mathcal{L}_{A,B}(s, s') &\equiv \exp(g_\theta(s)) [\|M_A\|^2 + \|M_B\|^2 + 2M'_A \cdot M_B] \quad (3.28)
 \end{aligned}$$

$$1177 \quad \mathcal{L}_g(s, s') \equiv (g_\theta(s) - [\|M_A\|^2 + \|M_B\|^2 + 2M'_A \cdot M_B])^2 \quad (3.29)$$

1178 where  $\cdot$  is the dot product. With tabular  $g$ , this sequence of operations should be  
 1179  $\mathcal{O}(mk)$ , which is much quicker than the naive  $\mathcal{O}(mk^2)$ .

### 1180 3.4.5 POP-Q-Learning

1181 Thus far, we have focused on Markov Reward Processes. For RL problems, we  
 1182 need to extend this approach to Markov Decision Processes (MDPs). An MDP  
 1183 is a tuple,  $(\mathcal{S}, \mathcal{A}, P, R, \gamma)$ , with state space  $\mathcal{S}$ , probabilistic transition function  
 1184  $P : \mathcal{S} \times \mathcal{A} \times \mathcal{S} \rightarrow \mathbb{R}_+$ , reward function  $R : \mathcal{S} \times \mathcal{A} \rightarrow \mathbb{R}$ , and discount factor  $\gamma \in [0, 1]$ .  
 1185 The goal in this setting is to find a probabilistic policy  $\pi : \mathcal{S} \times \mathcal{A} \rightarrow \mathbb{R}_+$  that maximizes  
 1186 the future discounted reward:

$$1187 \quad \pi^* = \arg \max_{\pi} \mathbb{E}_{\pi} \left[ \sum_{t=0}^{\infty} \gamma^t R(s_t, a_t) \right] \quad (3.30)$$

1188 Many RL methods use some variation of Q-learning [58, 38, 15, 26], which involves  
 1189 learning a state-action value function commonly called a  $Q$ -function:

$$1190 \quad Q^\pi(s, a) = \mathbb{E}_{\pi} \left[ \sum_{t=0}^{\infty} \gamma^t R(s_t, a_t) \mid s_0 = s, a_0 = a \right] \quad (3.31)$$

1191 By considering a fixed policy  $\pi$ , a combined state-space  $\mathcal{X} = \mathcal{S} \times \mathcal{A}$ , and a policy-  
 1192 conditioned transition function  $\tilde{P}^\pi((s, a), (s', a')) = P(s, a, s')\pi(s', a')$ , any MDP

---

**Algorithm 1** Deep POP-Q-Learning

---

Initialize Q-function,  $Q_{\theta^Q}$ , g-function,  $g_{\theta^g}$ , dual variable vector  $y$ , and some policy  $\pi_{\theta^\pi}$ .

**for** step  $t$  in  $1, \dots, N$  **do**

Sample mini-batch  $(s, a, r, s') \sim \mu$ .

Sample  $\tilde{a} \sim \pi_{\theta^\pi}(s), \tilde{a}' \sim \pi_{\theta^\pi}(s')$ .

# Compute features from penultimate layer of Q-network:

$\phi \leftarrow Q_{\theta^Q}(s, a), \phi' \leftarrow Q_{\theta^Q}(s', \tilde{a}')$ .

# Update g-function and dual variable vectors:

$\theta_t^g \leftarrow \theta_{t-1}^g - \eta_g \nabla_{\theta^g} \mathcal{L}_g(s, s')$

$A_t \leftarrow A_{t-1} - \eta_A \nabla_A \mathcal{L}_A(s, s')$

$B_t \leftarrow B_{t-1} - \eta_B \nabla_B \mathcal{L}_B(s, s')$

# Update Q-function using re-weighted Q-loss update:

$\theta_t^Q \leftarrow \theta_{t-1}^Q - \eta_Q \exp(g_{\theta^g}(s, a)) \nabla_{\theta^Q} \mathcal{L}_Q(\theta^Q)$

# Update policy with SAC-style loss:

$\theta_t^\pi \leftarrow \theta_{t-1}^\pi - \eta_\pi \nabla_{\theta^\pi} [Q_{\theta^Q}(s, \tilde{a}) - \log \pi_{\theta^\pi}(\tilde{a}|s)]$

**end for**

---

1193 reduces to a Markov Chain. Thus, as long as the NEC is satisfied in this modified  
1194 state-space, we can bound the approximation error of the Q-function. See Section 3.4.5  
1195 for a detailed derivation.

1196 Finally, for our method to applied to modern deep RL problems, we must extend our  
1197 approach to non-linear Q-functions. To do so, we approximate the Q-function with a  
1198 neural network,  $Q_{\theta^Q}$  parameterized by  $\theta^Q$  and consider a stochastic parameterized  
1199 policy  $\pi_{\theta^\pi}$ . To update  $Q_{\theta^Q}$ , we used a squared Bellman loss,  $\mathcal{L}_Q(\theta^Q) = (Q_{\theta^Q}(s, a) -$   
1200  $r - \gamma Q_{\theta^Q}(s', \pi_{\theta^\pi}(s')))^2$ , which we reweigh with  $\exp(g(s))$  as before. For our offline  
1201 RL experiments, we also add CQL regularization [26] to our Q-learning updates to  
1202 prevent over-optimism on low-support regions of the state-action space. To update  
1203 our linear dual variables  $y$ , we use the penultimate layer of  $Q_{\theta^Q}$  as our feature vector.  
1204 Finally, we use a SAC-style entropy regularized loss to update our policy network,  
1205  $\pi_{\theta^\pi}$ . Algorithm 1 provides an overview of our method.

## 1206 3.5 Experiments and Discussion

1207 We first apply POP-TD to a well-understood example so that we can directly illustrate  
1208 the how it resamples TD updates to a “safe” distribution. We use the simple three-  
1209 state task from Figure 3.2, including the specified transition function, value function,  
1210 and basis. Since this is a policy evaluation task, there is no policy to be separately  
1211 learned.

1212 For illustration purposes, we select the family of distributions  $\pi = (h/2, h/2, 1 - h)$   
1213 parameterized by  $h \in [0, 1]$ . This characterizes the possible distributions of data  
1214 that we will present to POP-TD and naive TD in this experiment. The on-policy  
1215 distribution corresponds to  $h_o \approx 0.51$ , and divides the family of distributions into  
1216 a left subset ( $h \leq h_o$ ) where the NEC holds and a right subset ( $h > h_o$ ) where it  
1217 does not. This is immediately apparent in Figure 3.2, where we plot the error at  
1218 convergence from running naive- and POP-TD above, and the effective distribution  
1219 of TD updates after reweighing below. In the left subset, where the NEC holds,  
1220 POP-TD does not resample TD updates at all. Therefore, the error of POP-TD  
1221 tracks naive TD (top), and the effective distribution of TD updates in POP-TD and  
1222 naive TD are the same as the data distribution (bottom).

1223 In the right subset, we observe that naive TD converges to poor solutions with  
1224 large error while POP-TD is able to learn with low error. Directly computing the  
1225 effective distribution, we see that naive TD adheres to the data distribution but  
1226 POP-TD resamples the TD updates. Looking at the behavior of POP-TD in the  
1227 right subset, we see that POP-TD resamples updates to the on-policy distribution  
1228  $p_o$  in  $p \in [p_o, 0.9]$ , corresponding to the horizontal segment. This allows the learned  
1229 Q-function to have very low error in that domain. As the data distribution becomes  
1230 more extreme ( $p \in [0.9, 1)$ ), POP-TD is not quite able to learn the resampling ratio,  
1231 and so the effective distribution shifts away from  $p_o$ . This leads to a corresponding  
1232 slight increase in error at extreme ratios. From this we observe that POP-TD requires  
1233 full support of the sampling distribution, similar to many offline RL algorithms [26,  
1234 47].

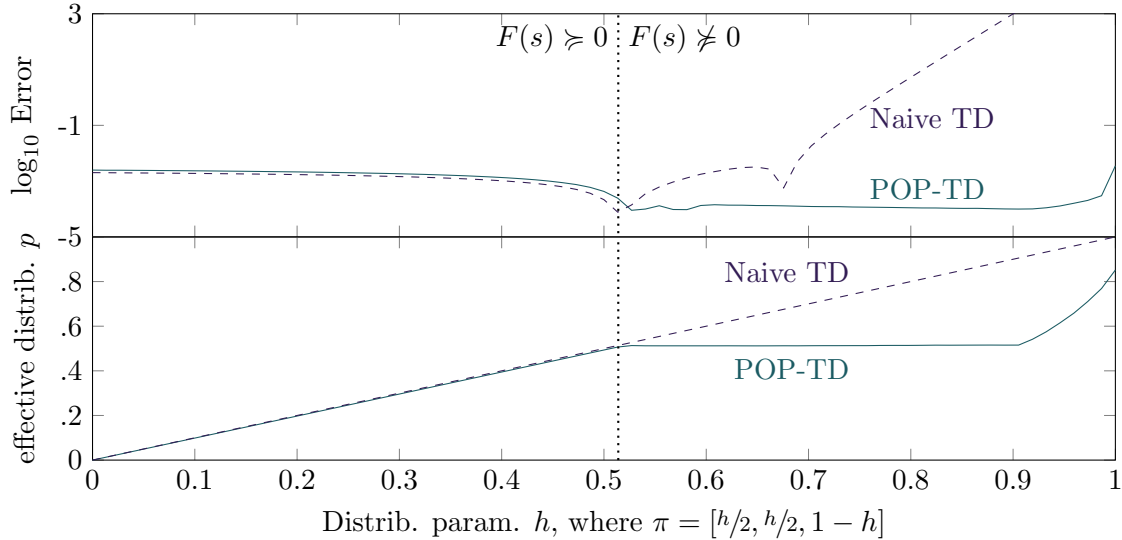


Figure 3.2: The error in the learned value function by naive- and POP-TD, plotted against a varying sampling distribution. In the left half of the plot, the NEC holds, and so POP-TD tracks the error of naive TD closely. In the right half of the plot naive TD diverges, while POP-TD resamples the data to a “safe” distribution and does not diverge.

1235 This simple experiment cleanly illustrates how POP-TD resamples TD updates to  
 1236 come from a “safe” distribution, and how that can greatly reduce the error in a policy  
 1237 evaluation task.

### 1238 3.5.1 POP-Q on GridWorld

1239 In this experiment, we consider the the simple grid environment from Figure 3.1,  
 1240 modified to add transitions from terminating states to the starting state. Our goal  
 1241 is to approximate the true Q-function with minimal error. Our training data is  
 1242 sampled following the suboptimal data policy ( $\bullet\bullet\bullet$ ), adding uniform random dithering  
 1243 to guarantee that every state-action pair is represented. We represent the Q-function  
 1244 as a linear function with a fixed random basis  $\Phi \in \mathbb{R}^{64 \times 53}$ , training it to convergence  
 1245 using naive Q-learning and linear POP-Q separately. For POP-Q, we also randomly  
 1246 initialize matrices  $A, B \in \mathbb{R}^{53 \times 4}$  and a tabular  $g \in \mathbb{R}^{64}$  separately. (We will later

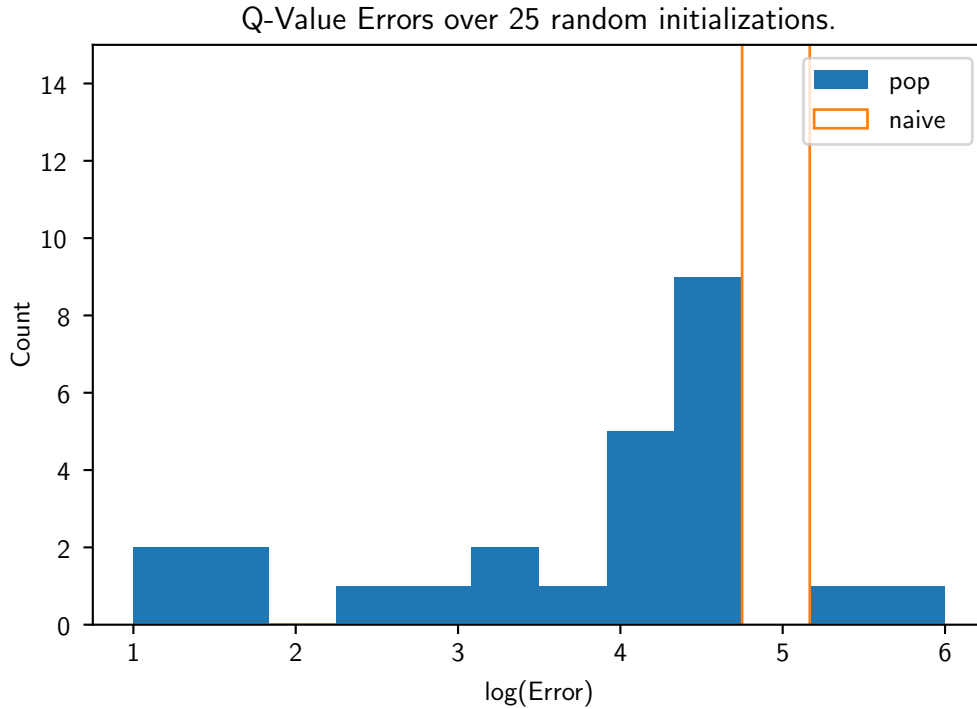


Figure 3.3: Log Q-function errors for naive and POP Q-Learning on Figure 3.1, over 25 randomly sampled bases. Errors are computed using a tabular  $g$  function, and bins are exponentially wide. POP-Q substantially reduces error in most of the sampled bases.

1247 consider an approximate  $g$ .)

1248 **Setting the rank of  $A, B$ :** We could simply set the rank of  $A$  and  $B$  as any other  
 1249 hyperparameter, but since this problem is sufficiently small we can instead compute  
 1250 the minimum rank directly. To do this, we compute the degree of rank deficiency of  
 1251 the matrix  $\mathbb{E}_s[F(s)]$  from Equation (3.8) on our dataset, and set the rank of  $A$  and  
 1252  $B$  so the sum of the rank of  $\mathbb{E}_s[F(s)]$  and  $A$  and  $B$  is at least  $k$ . For this example,  
 1253 for  $k = 53$ , we find that  $\text{rank}(A) = \text{rank}(B) = 4$  is sufficient for this example.

1254 **Results with an exact, tabular  $g$**

1255 Since tabular Q-learning always converges to the global optimum [58], we use that to  
1256 compute the ground-truth Q-function. All error reported is relative to that assumed  
1257 ground truth.

1258 Figure 3.3 shows the distribution of errors achieved by vanilla and POP Q-learning  
1259 over 25 different bases on our task. Vanilla Q-learning performs consistently poorly,  
1260 achieving a (large) amount of error at all seeds. This is expected because we have  
1261 deliberately engineered the task to be unstable. In comparison, POP-TD improves  
1262 performance over most seeds, and in some cases enables near-perfect fitting of the  
1263 Q-function.

1264 Throughout this chapter we have drawn a distinction between importance sam-  
1265 pling/Emphatic TD methods and our work. While the former attempts to resample  
1266 to the on-policy distribution, our work seeks to resample to the closest stable distribu-  
1267 tion. We illustrate this difference in Figure 3.4, where we display the rates at which  
1268 states are visited in our GridWorld. The distribution in our dataset (top-right) is far  
1269 from the on-policy distribution (top-left), which is what importance sampling and  
1270 Emphatic methods will attempt to resample to. In comparison, POP-Q resamples  
1271 minimally (bottom row), where the effective distribution reached is very close to the  
1272 data distribution.

1273 **Results with an approximate, linear  $g$**

1274 The current experiments with POP-Q learning all use a tabular  $g$ . This works, but  
1275 takes the same memory as would learning a tabular value function, which would  
1276 provably converge to the global optimum (side-stepping the entire problem). A key  
1277 step in adopting POP-Q is ensuring that all parameters are at most order  $\mathcal{O}(k)$  (i.e.  
1278 comparable to the size of the learned weights) and are therefore learnable with the  
1279 same order of time and space as regular TD. We also wish to (eventually) exploit the  
1280 generalization afforded to us by neural networks, to hopefully learn more accurate  
1281 models with less data.

1282 The matrices  $A$  and  $B$  are sized  $k \times m$ , where  $m \ll k$ , and so are sufficiently  
1283 small. We now need to approximate  $g$  as a linear function with fixed bases vectors  
1284  $\Phi_g = (\phi_{g,1}, \phi_{g,2}, \dots, \phi_{g,n})$ ,  $\phi_{g,o} \in \mathbb{R}^l$  and learned weights  $w_g \in \mathbb{R}^l$  of size  $l < n$ :

$$1285 \qquad g(s) = \phi_{g,s} \cdot w_g \qquad (3.32)$$

1286 To understand the relationship between the degree of approximation (as measured by  
1287 the size of the basis  $l$ ) and the performance of our system, we initialize 25 different  
1288  $n \times n$  bases and report the performance as the bases are truncated down from 64 to  
1289 1. This is illustrated in Figure 3.5.

1290 Figure 3.5 reveals that the performance of POP-Q is (as expected) sensitive to the  
1291 exact basis chosen. For some bases, the error increases with only a small amount of  
1292 approximation, but for some “lottery-ticket” bases, this continues to work even as  
1293 the bases are truncated to rank 1. For some bases, this continues to work despite  
1294 extreme approximation is because the degree of resampling required is minimal and  
1295 the system is fairly easy to resample.

1296 **A note on initialization** When performing experiments, we note that the perfor-  
1297 mance of POP-TD depends sharply on the condition number of  $\Phi$ , but not necessarily  
1298 that of  $\Phi_g$ . Specifically, we see that an orthogonal initialization step on  $\Phi$  is crucial for  
1299 performance. (In this step we set  $\Phi$  to the orthogonal matrix of the QR-decomposition  
1300 of a matrix where entries are sampled uniformly at random.) We conjecture that this  
1301 happens because POP-TD seeks to stochastically learn  $\Phi^T A \Phi$ , and a poor condition  
1302 number of  $\Phi$  leads to values that span multiple orders of magnitude and linear  
1303 approximation is known to perform poorly on such data.

## 1304 3.6 Conclusion

1305 In this chapter we introduced POP-TD, a method for effective TD learning under  
1306 off-policy distributions, with applications to offline RL and learning under large  
1307 distribution shifts. Unlike existing emphatic TD and importance sampling methods

1308 which resample to the on-policy distribution, POP-TD resamples to the closest  
1309 distribution under which TD will provably not diverge.

1310 We present POP-TD on an existing “deadly triad” example in the literature, showing  
1311 how the resampling process operates in theory. We extend this to a more general  
1312 GridWorld-style Q-learning task which diverges under vanilla TD, but is consistently  
1313 solved by POP-Q-learning.

1314 A key strength of POP-Q-learning is that it achieves all this with a per-loop com-  
1315 pute and memory overhead of the same order as Q-learning methods, and can be  
1316 implemented and optimized in the same loop as any TD or Q-learning method. In  
1317 this sense, it offers a cheap mechanism to stabilize off-policy TD, particularly in the  
1318 context of offline RL.

1319 A possible future expansion of this project is to integrate this with an existing  
1320 offline RL method such as Conservative Q-Learning (CQL) and examine whether this  
1321 improves performance. We propose CQL specifically because it constrains actions  
1322 to remain within the support of the data, but does not explicitly constrain the  
1323 distribution of states to minimize distribution shift. POP methods require adequate  
1324 support (which CQL provides), and in turn are able to minimize distribution shift.  
1325 This suggests that the two algorithms may have some symbiotic relationship.

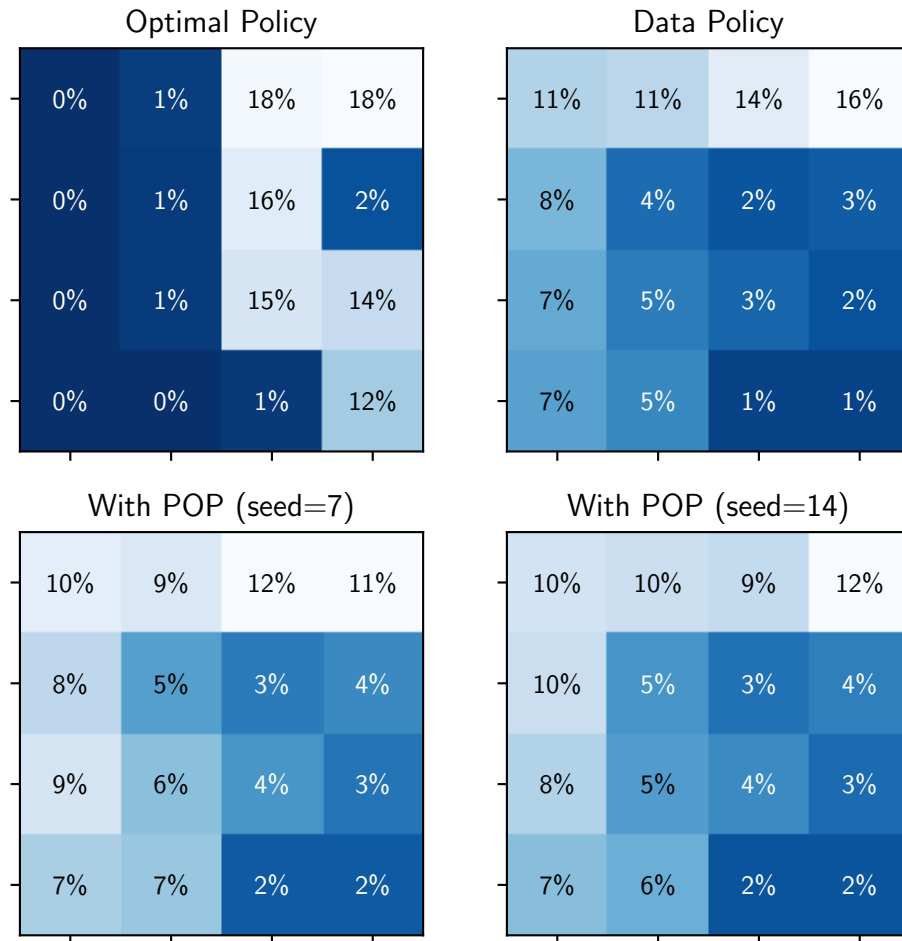


Figure 3.4: Rates at which states are visited in GridWorld. On the top row, we show how the optimal policy (left) is very far from the data policy (right). On the bottom row, we show the effective distribution after POP-Q resamples the data. The effective distribution is very close to the data distribution, despite the tremendous improvement in error.

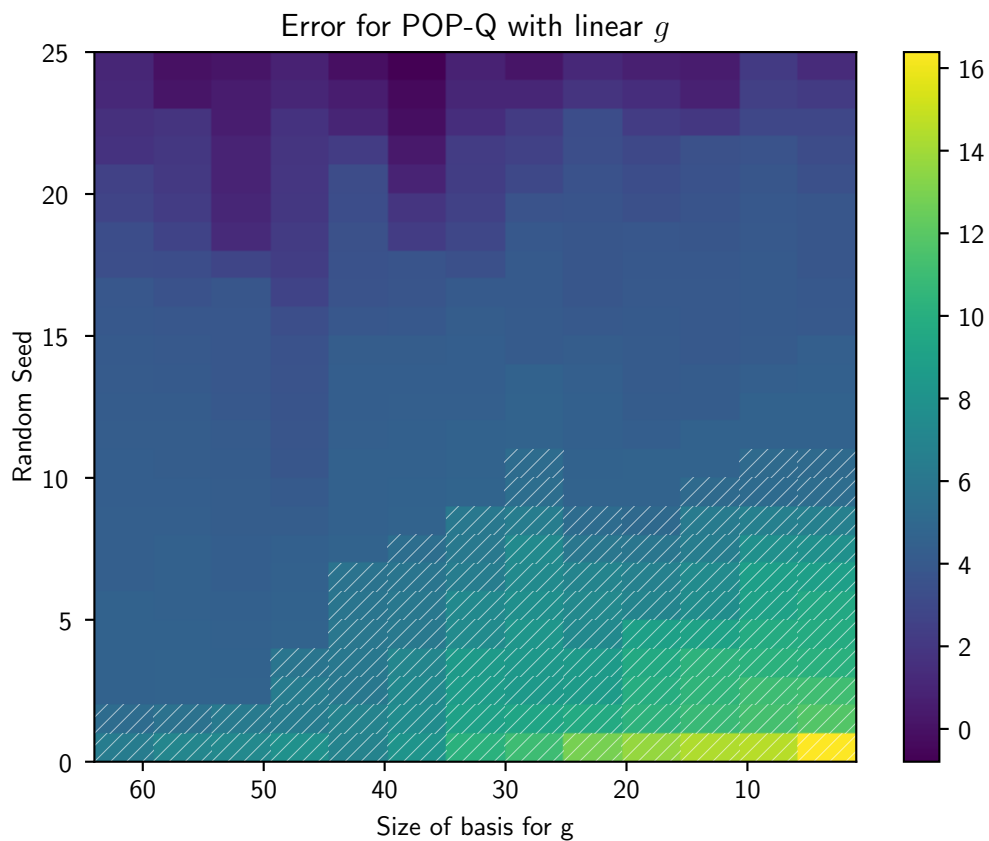


Figure 3.5: Error for POP-Q with linear  $g$  functions. Each row corresponds to one starting basis, and each column corresponds to a basis size  $l$  as it is reduced from 64 to 1. The hatched cells correspond to combinations of seeds and bases in which POP-Q performs worse than vanilla Q-learning. Under linear approximation POP-Q greatly improves performance over vanilla TD.

# Conclusion

1326

1327 We have examined two notions of stability with a subtle relationship: that of learned  
1328 dynamics models, and the training of reinforcement learning algorithms. In doing  
1329 so, we have introduced new techniques in both areas, as well as filled in a gap in the  
1330 literature on the unsuitability of regularization to solve instability in RL.

1331 One key gap in the RL literature that we hope to address in the future is how we  
1332 should regularize deep RL in a principled manner. While our prior work shows that  
1333 simple  $\ell_2$  regularization can cause divergence, the literature is ripe for either adaptive  
1334 regularization schemes that can detect and avoid pathological behavior, or for novel  
1335 non-convex regularizations that fail similarly.

1336 Separately, there remains a large gap in a key area within offline RL in dealing with  
1337 the distributional shift problem. While there have been many recent advances in the  
1338 field, these advances have been largely incremental, and the field remains ripe for  
1339 a novel perspective that can address this. We propose that POP-TD is that novel  
1340 perspective. Unlike the existing literature, the key insight that POP-TD brings to  
1341 the field is that we can resample to “safe” off-policy distributions that are close to  
1342 the data distribution, instead of the on-policy distribution which may be arbitrarily  
1343 far. With these novel POP techniques, we hope to allow offline RL to resample the  
1344 data as little as possible to avoid instability from large resampling coefficients, and  
1345 learn to generalize from a set of diverse and possibly even adversarial experts that  
1346 complete tasks in mutually incompatible ways.



# Notation and Definitions

1348 Standard notation for RL concepts through this thesis.

Symbol	Description
$n \in \mathbb{Z}^+$	Number of states.
$k \in \mathbb{Z}^+$	Number of features in the value basis.
$\pi \in \mathbb{R}^n$	on-policy distribution.
$\mu \in \mathbb{R}^n$	sampling distribution, may be on- or off-policy.
$\Phi \in \mathbb{R}^{[n \times k]}$	Feature basis for the value function
$\hat{w} \in \mathbb{R}^{[k \times 1]}$	Linear weights for value function, fit using least-squares regression of $V$ on $\Phi$ .
$w^*(\eta) \in \mathbb{R}^{[k \times 1]}$	Linear weights for value function, learned using TD.
$\Phi w^*(\eta) \in \mathbb{R}^{[n \times 1]}$	Learned value function
$V \in \mathbb{R}^{[n \times 1]}$	True value function
$\ V\  \in \mathbb{R}$	Error from guessing zeros, equivalent to the threshold for a vacuous example
$\ x\  \in \mathbb{R}_0^+$	$\ell_2$ -norm of vector or matrix $x$ , equal to $\sqrt{x^\top x}$
$\ x\ _D \in \mathbb{R}_0^+$	$\ell_2$ -norm of vector or matrix $x$ under $D$ , equal to $\sqrt{x^\top D x}$

1349 **Regularization**

Symbol	Description
$\eta \in \mathbb{R}_0^+$	$\ell_2$ regularization parameter
$h \in [0, 1]$	distribution parameter used to express a family of possible sampling distributions.
$\eta_m \in \mathbb{R}_0^+$	$\ell_2$ regularization parameter for emphasis model in COF-PAC (the Emphatic algorithm we analyze)
$\eta_v \in \mathbb{R}_0^+$	$\ell_2$ regularization parameter for value model in COF-PAC (the Emphatic algorithm we analyze)
$v : \mathbb{R}^+ \rightarrow \mathbb{R}^n$	apparent distribution induced by $\eta$ -regularizing the emphatic correction of off-policy $\mu$ to on-policy $\pi$

1350 **Projected Off-Policy**

Symbol	Description
$m \in \mathbb{Z}^+$	Number of features in the $g$ -basis (for POP methods).
$l \in \mathbb{Z}^+$	Rank of $A$ and $B$ two-timescales parameters (for POP methods).
$g : \mathcal{S} \rightarrow \mathbb{R}$	dual objective component, learned opposite $A$ and $B$ in POP methods.
$e^{g(s)} \in \mathbb{R}^+$	The resampling coefficient for TD updates from state $s$
$\Phi_g \in \mathbb{R}^{[n \times m]}$	Feature basis for the learned linear $g$ function
$w_g \in \mathbb{R}^{[m \times 1]}$	Linear weights for learned $g$ function
$A, B \in \mathbb{R}^{[k \times l]}$	Two-timescales parameters learned alongside $g$ in POP methods, where $l \ll k$ .
$\Phi_g w_g \in \mathbb{R}^{[n \times 1]}$	Learned $g$ function

1351

# Bibliography

- 1352 [1] Brandon Amos, Lei Xu, and J Zico Kolter. “Input convex neural networks”. In:  
1353 *Proceedings of the 34th International Conference on Machine Learning-Volume*  
1354 *70*. JMLR.org. 2017, pp. 146–155.
- 1355 [2] Caroline Blocher, Matteo Saveriano, and Dongheui Lee. “Learning stable dynam-  
1356 ical systems using contraction theory”. In: *2017 14th International Conference*  
1357 *on Ubiquitous Robots and Ambient Intelligence (URAI)*. IEEE. 2017, pp. 124–  
1358 129.
- 1359 [3] Byron Boots, Geoffrey J Gordon, and Sajid M Siddiqi. “A constraint generation  
1360 approach to learning stable linear dynamical systems”. In: *Advances in neural*  
1361 *information processing systems*. 2008, pp. 1329–1336.
- 1362 [4] Samuel Burer and Renato DC Monteiro. “A nonlinear programming algorithm  
1363 for solving semidefinite programs via low-rank factorization”. In: *Mathematical*  
1364 *Programming* 95.2 (2003), pp. 329–357.
- 1365 [5] Yize Chen, Yuanyuan Shi, and Baosen Zhang. “Optimal Control Via Neural  
1366 Networks: A Convex Approach”. In: *arXiv preprint arXiv:1805.11835* (2018).
- 1367 [6] Yinlam Chow et al. “A lyapunov-based approach to safe reinforcement learning”.  
1368 In: *Advances in Neural Information Processing Systems*. 2018, pp. 8092–8101.
- 1369 [7] Jonas Degraeve et al. “Magnetic control of tokamak plasmas through deep  
1370 reinforcement learning”. In: *Nature* 602.7897 (2022), pp. 414–419.
- 1371 [8] Raghuram Bharadwaj Diddigi, Chandramouli Kamanchi, and Shalabh Bhatna-  
1372 gar. “A convergent off-policy temporal difference algorithm”. In: *arXiv preprint*  
1373 *arXiv:1911.05697* (2019).

- 1374 [9] Simon S Du et al. “Stochastic variance reduction methods for policy evaluation”.  
1375 In: *International Conference on Machine Learning*. PMLR. 2017, pp. 1049–1058.
- 1376 [10] William Fedus et al. “Revisiting fundamentals of experience replay”. In: *Inter-*  
1377 *national Conference on Machine Learning*. PMLR. 2020, pp. 3061–3071.
- 1378 [11] Scott Fujimoto, David Meger, and Doina Precup. “Off-policy deep reinforcement  
1379 learning without exploration”. In: *International conference on machine learning*.  
1380 PMLR. 2019, pp. 2052–2062.
- 1381 [12] Yarin Gal, Rowan McAllister, and Carl Edward Rasmussen. “Improving PILCO  
1382 with Bayesian neural network dynamics models”. In: *Data-Efficient Machine*  
1383 *Learning workshop, ICML*. Vol. 4. 2016.
- 1384 [13] Carles Gelada and Marc G Bellemare. “Off-policy deep reinforcement learning  
1385 by bootstrapping the covariate shift”. In: *Proceedings of the AAAI Conference*  
1386 *on Artificial Intelligence*. Vol. 33. 01. 2019, pp. 3647–3655.
- 1387 [14] Shixiang Gu et al. “Continuous deep q-learning with model-based acceleration”.  
1388 In: *International Conference on Machine Learning*. 2016, pp. 2829–2838.
- 1389 [15] Tuomas Haarnoja et al. “Soft actor-critic: Off-policy maximum entropy deep  
1390 reinforcement learning with a stochastic actor”. In: *International conference on*  
1391 *machine learning*. PMLR. 2018, pp. 1861–1870.
- 1392 [16] Assaf Hallak and Shie Mannor. “Consistent on-line off-policy evaluation”. In:  
1393 *International Conference on Machine Learning*. PMLR. 2017, pp. 1372–1383.
- 1394 [17] Hado van Hasselt et al. “Expected eligibility traces”. In: *arXiv preprint arXiv:2007.01839*  
1395 (2021).
- 1396 [18] Kaiming He et al. “Delving deep into rectifiers: Surpassing human-level perfor-  
1397 mance on imagenet classification”. In: *Proceedings of the IEEE international*  
1398 *conference on computer vision*. 2015, pp. 1026–1034.
- 1399 [19] Ray Jiang et al. “Learning Expected Emphatic Traces for Deep RL”. In: *arXiv*  
1400 *preprint arXiv:2107.05405* (2021).
- 1401 [20] Hassan K Khalil and Jessy W Grizzle. *Nonlinear systems*. Vol. 3. Prentice hall  
1402 Upper Saddle River, NJ, 2002.

- 1403 [21] S Mohammad Khansari-Zadeh and Aude Billard. “Learning stable nonlinear  
1404 dynamical systems with gaussian mixture models”. In: *IEEE Transactions on*  
1405 *Robotics* 27.5 (2011), pp. 943–957.
- 1406 [22] Rahul Kidambi et al. “Morel: Model-based offline reinforcement learning”. In:  
1407 *Advances in neural information processing systems* 33 (2020), pp. 21810–21823.
- 1408 [23] Diederik P Kingma and Max Welling. “Auto-encoding variational bayes”. In:  
1409 *arXiv preprint arXiv:1312.6114* (2013).
- 1410 [24] J Kolter. “The fixed points of off-policy TD”. In: *Advances in Neural Information*  
1411 *Processing Systems* 24 (2011), pp. 2169–2177.
- 1412 [25] Aviral Kumar, Abhishek Gupta, and Sergey Levine. “Discor: Corrective feed-  
1413 back in reinforcement learning via distribution correction”. In: *arXiv preprint*  
1414 *arXiv:2003.07305* (2020).
- 1415 [26] Aviral Kumar et al. “Conservative Q-Learning for Offline Reinforcement Learn-  
1416 ing”. In: *Advances in Neural Information Processing Systems 33: Annual Con-*  
1417 *ference on Neural Information Processing Systems 2020, NeurIPS 2020, De-*  
1418 *cember 6-12, 2020, virtual*. Ed. by Hugo Larochelle et al. 2020. URL: [https://](https://proceedings.neurips.cc/paper/2020/hash/0d2b2061826a5df3221116a5085a6052-Abstract.html)  
1419 [proceedings.neurips.cc/paper/2020/hash/0d2b2061826a5df3221116a5085a6052-](https://proceedings.neurips.cc/paper/2020/hash/0d2b2061826a5df3221116a5085a6052-Abstract.html)  
1420 [Abstract.html](https://proceedings.neurips.cc/paper/2020/hash/0d2b2061826a5df3221116a5085a6052-Abstract.html).
- 1421 [27] Aviral Kumar et al. “DR3: Value-Based Deep Reinforcement Learning Requires  
1422 Explicit Regularization”. In: *International Conference on Learning Representa-*  
1423 *tions*. 2022. URL: <https://openreview.net/forum?id=P0vMvLi91f>.
- 1424 [28] Aviral Kumar et al. “Stabilizing off-policy q-learning via bootstrapping error  
1425 reduction”. In: *Advances in Neural Information Processing Systems* 32 (2019).
- 1426 [29] Joseph La Salle and Solomon Lefschetz. *Stability by Liapunov’s Direct Method*  
1427 *with Applications by Joseph L Salle and Solomon Lefschetz*. Vol. 4. Elsevier,  
1428 2012.
- 1429 [30] Sergey Levine et al. “Offline Reinforcement Learning: Tutorial, Review, and  
1430 Perspectives on Open Problems”. In: *CoRR* abs/2005.01643 (2020). arXiv:  
1431 2005.01643. URL: <https://arxiv.org/abs/2005.01643>.

- 1432 [31] Sergey Levine et al. “Offline Reinforcement Learning: Tutorial, Review, and  
1433 Perspectives on Open Problems”. In: *CoRR* abs/2005.01643 (2020). arXiv:  
1434 2005.01643. URL: <https://arxiv.org/abs/2005.01643>.
- 1435 [32] Qiang Liu et al. “Breaking the curse of horizon: Infinite-horizon off-policy  
1436 estimation”. In: *Advances in Neural Information Processing Systems* 31 (2018).
- 1437 [33] Sridhar Mahadevan et al. “Proximal reinforcement learning: A new theory of se-  
1438 quential decision making in primal-dual spaces”. In: *arXiv preprint arXiv:1405.6757*  
1439 (2014).
- 1440 [34] Gaurav Manek and J Zico Kolter. “Learning stable deep dynamics models”. In:  
1441 *Advances in neural information processing systems* 32 (2019).
- 1442 [35] Gaurav Manek and J Zico Kolter. “The Pitfalls of Regularization in Off-Policy  
1443 TD Learning”. In: *Advances in Neural Information Processing Systems*. Ed.  
1444 by Alice H. Oh et al. 2022. URL: <https://openreview.net/forum?id=vK53GLZJes8>.
- 1445
- 1446 [36] Gaurav Manek, Melrose Roderick, and J Zico Kolter. “Projected Off-Policy TD  
1447 Learning Stabilize Offline Reinforcement Learning”. In: Jan. 2023.
- 1448 [37] Nikhil Mishra, Pieter Abbeel, and Igor Mordatch. “Prediction and control with  
1449 temporal segment models”. In: *Proceedings of the 34th International Conference*  
1450 *on Machine Learning-Volume 70*. JMLR. org. 2017, pp. 2459–2468.
- 1451 [38] Volodymyr Mnih et al. “Human-level control through deep reinforcement learn-  
1452 ing”. In: *Nature* 518.7540 (Feb. 2015), pp. 529–533. ISSN: 00280836. URL: <http://dx.doi.org/10.1038/nature14236>.
- 1453
- 1454 [39] Ofir Nachum et al. “Algaedice: Policy gradient from arbitrary experience”. In:  
1455 *arXiv preprint arXiv:1912.02074* (2019).
- 1456 [40] Ofir Nachum et al. “Dualdice: Behavior-agnostic estimation of discounted sta-  
1457 tionary distribution corrections”. In: *Advances in Neural Information Processing*  
1458 *Systems* 32 (2019).
- 1459 [41] Anusha Nagabandi et al. “Neural network dynamics for model-based deep  
1460 reinforcement learning with model-free fine-tuning”. In: *2018 IEEE International*  
1461 *Conference on Robotics and Automation (ICRA)*. IEEE. 2018, pp. 7559–7566.

- 1462 [42] Antonis Papachristodoulou and Stephen Prajna. “On the construction of Lyapunov functions using the sum of squares decomposition”. In: *Proceedings of the 41st IEEE Conference on Decision and Control, 2002*. Vol. 3. IEEE. 2002, pp. 3482–3487.
- 1463
- 1464
- 1465
- 1466 [43] Pablo A Parrilo. “Structured semidefinite programs and semialgebraic geometry methods in robustness and optimization”. PhD thesis. California Institute of Technology, 2000.
- 1467
- 1468
- 1469 [44] Doina Precup. “Eligibility traces for off-policy policy evaluation”. In: *Computer Science Department Faculty Publication Series* (2000), p. 80.
- 1470
- 1471 [45] Spencer M Richards, Felix Berkenkamp, and Andreas Krause. “The Lyapunov neural network: Adaptive stability certification for safe learning of dynamic systems”. In: *arXiv preprint arXiv:1808.00924* (2018).
- 1472
- 1473
- 1474 [46] Arno Schödl et al. “Video textures”. In: *Proceedings of the 27th annual conference on Computer graphics and interactive techniques*. ACM Press/Addison-Wesley Publishing Co. 2000, pp. 489–498.
- 1475
- 1476
- 1477 [47] Laixi Shi et al. “Pessimistic q-learning for offline reinforcement learning: Towards optimal sample complexity”. In: *arXiv preprint arXiv:2202.13890* (2022).
- 1478
- 1479 [48] Richard S Sutton and Andrew G Barto. *Reinforcement learning: An introduction*. Second Edition. MIT press, 2020.
- 1480
- 1481 [49] Richard S Sutton, A Rupam Mahmood, and Martha White. “An emphatic approach to the problem of off-policy temporal-difference learning”. In: *The Journal of Machine Learning Research* 17 (2016), pp. 2603–2631.
- 1482
- 1483
- 1484 [50] Richard S Sutton et al. “Fast gradient-descent methods for temporal-difference learning with linear function approximation”. In: *Proceedings of the 26th Annual International Conference on Machine Learning*. 2009, pp. 993–1000.
- 1485
- 1486
- 1487 [51] Andrew J Taylor et al. “Episodic Learning with Control Lyapunov Functions for Uncertain Robotic Systems”. In: *arXiv preprint arXiv:1903.01577* (2019).
- 1488
- 1489 [52] Russ Tedrake. *Underactuated Robotics. Algorithms for Walking, Running, Swimming, Flying, and Manipulation*. 2023. URL: <https://underactuated.csail.mit.edu>.
- 1490
- 1491

- 1492 [53] Andrey Nikolayevich Tikhonov. “On the stability of inverse problems”. In: *Dokl.*  
1493 *Akad. Nauk SSSR*. Vol. 39. 1943, pp. 195–198.
- 1494 [54] JN Tsitsiklis and B Van Roy. “An analysis of temporal-difference learning  
1495 with function approximation”. In: *Rep. LIDS-P-2322*. *Lab. Inf. Decis. Syst.*  
1496 *Massachusetts Inst. Technol. Tech. Rep* (1996).
- 1497 [55] Jonas Umlauft and Sandra Hirche. “Learning stable stochastic nonlinear dynam-  
1498 ical systems”. In: *Proceedings of the 34th International Conference on Machine*  
1499 *Learning-Volume 70*. JMLR. org. 2017, pp. 3502–3510.
- 1500 [56] Jake VanderPlas. *Triple Pendulum CHAOS!* [http://jakevdp.github.io/  
1501 blog/2017/03/08/triple-pendulum-chaos/](http://jakevdp.github.io/blog/2017/03/08/triple-pendulum-chaos/). Mar. 2017.
- 1502 [57] Andrew J Wagenmaker et al. “First-Order Regret in Reinforcement Learning  
1503 with Linear Function Approximation: A Robust Estimation Approach”. In:  
1504 *Proceedings of the 39th International Conference on Machine Learning*. Ed. by  
1505 Kamalika Chaudhuri et al. Vol. 162. *Proceedings of Machine Learning Research*.  
1506 PMLR, July 2022, pp. 22384–22429. URL: [https://proceedings.mlr.press/  
1507 v162/wagenmaker22a.html](https://proceedings.mlr.press/v162/wagenmaker22a.html).
- 1508 [58] Christopher JCH Watkins and Peter Dayan. “Q-learning”. In: *Machine learning*  
1509 8.3 (1992), pp. 279–292.
- 1510 [59] Ronald J Williams and Leemon C Baird III. *Analysis of some incremental*  
1511 *variants of policy iteration: First steps toward understanding actor-critic learning*  
1512 *systems*. Tech. rep. Citeseer, 1993.
- 1513 [60] Yifan Wu, George Tucker, and Ofir Nachum. “Behavior regularized offline  
1514 reinforcement learning”. In: *arXiv preprint arXiv:1911.11361* (2019).
- 1515 [61] Huizhen Yu. “On convergence of some gradient-based temporal-differences  
1516 algorithms for off-policy learning”. In: *arXiv preprint arXiv:1712.09652* (2017).
- 1517 [62] Tianhe Yu et al. “Mopo: Model-based offline policy optimization”. In: *Advances*  
1518 *in Neural Information Processing Systems* 33 (2020), pp. 14129–14142.
- 1519 [63] Shangdong Zhang, Hengshuai Yao, and Shimon Whiteson. “Breaking the Deadly  
1520 Triad with a Target Network”. In: *CoRR* abs/2101.08862 (2021). arXiv: 2101.  
1521 08862. URL: <https://arxiv.org/abs/2101.08862>.

- 1522 [64] Shangtong Zhang et al. “Provably convergent two-timescale off-policy actor-  
1523 critic with function approximation”. In: *International Conference on Machine*  
1524 *Learning*. PMLR. 2020, pp. 11204–11213.